Send Orders for Reprints to reprints@benthamscience.net

Current Pharmaceutical Design, **2014,** *20,* **000-000** **1**

PET Radioligands for *In Vivo* Visualization of Neuroinflammation

Dieter Ory[a], Sofie Celen[a], Alfons Verbruggen[a] and Guy Bormans[a,*]

[a]*Laboratory for Radiopharmacy, KU Leuven, Leuven, Belgium*

Abstract: Neuroinflammation is a well-orchestrated, dynamic, multicellular process playing a major role in neurodegenerative disorders. The microglia which make up the innate immune system of the central nervous system are key cellular mediators of neuroinflammatory processes. In normal condition they exert a protective function, providing tissue repair by releasing anti-inflammatory cytokines and neurotrophic factors. Upon neuronal injury or infection, they become overactivated, thereby releasing neurotoxic substances, amplifying neuroinflammation leading to neurodegeneration. Positron emission tomography (PET) provides a sensitive non-invasive imaging technique to study and quantify receptor and enzyme expression. A radiolabeled tracer for a protein (over)expressed in neuroinflammation and more specifically for the overactivated microglia would be useful as a diagnostic tool in the follow-up of neuroinflammation progression and to study the efficacy of anti-inflammatory therapy over time. In this manuscript, an overview of potential PET tracer targets upregulated during neuroinflammation is provided together with the current radiotracers used to image these targets. In addition, lead structures to develop radiotracers for new targets are suggested.

Keywords: Neuroinflammation, positron emission tomography.

1. INTRODUCTION

A. Neuroinflammation

Inflammation is an adaptive response for restoring tissue homeostasis and implies a tight interplay between a tissue and the immune system. Examples of classical inflammation include the response to bacterial, parasitic or viral infections. It is a multicellular process characterized by (1) changes in local vasculature (increased blood flow and vascular permeability), (2) activation of resident immune competent cells, (3) infiltration of mobile cells of the immune system (neutrophils, macrophages and lymphocytes) and (4) cytokine production [1,2]. Neuroinflammation is the inflammation as observed in central nervous system (CNS) diseases including stroke, multiple sclerosis (MS), amyotrophic lateral sclerosis (ALS), Parkinson's disease (PD), Alzheimer's disease (AD), Huntington's disease (HD), viral/bacterial infections, neoplasias and head traumas. These pathologies trigger an immune activation in the brain which on the one hand is involved in tissue repair and neuroregeneration, and on the other hand results in collateral damage to brain tissue, loss of neurons and dysfunction. Neuroinflammation is associated with autoimmune diseases (e.g. MS), acute (e.g. ischemia) or chronic (e.g. AD) CNS disease processes and CNS infections (e.g. herpes simplex virus type 1 encephalitis). Neuroinflammation arising in the absence of microorganisms has been termed sterile inflammation [2-4]. Graeber *et al.* even proposed to replace the term 'neuroinflammation' with the term 'microglial activation' since the vast majority of neuroinflammatory conditions do not fulfil the main criteria of inflammation [1].

Microglia are the major resident immune cells of the CNS and constitute up to 10% of the total cell population of the brain. They exert both neuroprotective and neurotoxic roles. As a consequence of CNS insults e.g. deposition of amyloid beta (Aβ), plaques or stroke, microglia become overactivated and change from a resting, ramified form to a reactive, amoeboid form. The reactive, amoeboid form enables microglia to function as phagocytes, expresses new surface markers, proliferates and releases a variety of cytokines and growth factors. Activation of microglial cells is mediated by pattern recognition receptors (PRRs) that bind to pathogen associated molecular patterns (PAMPs) or damage associated molecular patterns (DAMPs) which are expressed on cells that play main roles in innate immune responses, including macrophages and glial cells. Toll-like receptors (TLRs) are an example of PRRs. They recognise various PAMPs which are not present in the host. For instance, TLR4 recognises lipopolysaccharide (LPS) originating from gram-negative bacteria, whereas TLR3 recognises viral double-stranded RNA [4]. Receptors for advanced glycation end-products (RAGE) which are correlated with Aβ interaction in AD [5,6] and NOD-like receptors (NLRs) which act as pivotal sensors of infection and stress in intracellular compartments [7], are other examples of PRRs. Microglia and astrocytes also express purinergic receptors which respond to ATP released from cells during cell death, traumatic injury, or ischemia [4,8]. In addition, scavenger receptors which are involved in the uptake of several substances such as oxidized proteins, lipids, apoptotic cells and which probably contribute to cell signaling are also expressed on microglia and astrocytes [4,9]. These receptors are supposed to be capable of detecting PAMPs and DAMPs such as Aβ and LPS. Recognition by and ligation of PRRs results in activation of signal transduction pathways which regulate diverse transcriptional and posttranscriptional processes. These include activation of downstream kinases such as MAP kinase which in turn control multiple, signal dependent transcription factors including NF-κB. These transcription factors regulate expression of an important subset of highly induced genes including cytokines. Genes encoding proteins with antimicrobial activities and genes influencing protein synthesis, substrate metabolism, cell motility, phagocytosis, intracellular killing and antigen presentation are also induced.

This wide array of biological changes which occur in activated microglia results in a communication network between the cells of the CNS immune response. Depending on the way of activation, microglia can be classified in two main groups: the M1 phenotype or classically activated microglia and the M2 phenotype or alternatively activated microglia. The pro-inflammatory phenotype M1 is activated by IFN-ɣ produced by Th1 T-lymphocytes or signaling through TLRs. The anti-inflammatory phenotype M2 is activated by IL-4 and IL-13 produced by Th2 T-lymphocytes and other cell types. M1-type microglia produce TNF-α, IL-1β, IL-6, nitric oxide, superoxide, hydrogen peroxide and matrix metalloproteinases with the purpose to defend the host against pathogens and tumor cells but unfortunately, these mediators cause also damage to healthy host cells. Besides these direct effects, the release of pro-

*Address correspondence to this author at the Laboratory for Radiopharmacy, Campus Gasthuisberg O&N2, Herestraat 49 Box 821, BE-3000 Leuven, Belgium. Tel.: +32 16 330447; Fax: +32 16 330449;
E-mail: Guy.Bormans@pharm.kuleuven.be

1381-6128/14 $58.00+.00

inflammatory cytokines by M1-type microglia also leads to an amplification of the inflammatory response and even a more injurious accumulation of neurotoxins in CNS tissue. In contrast, M2-type microglia produce IL-10 and arginase-1 leading to tissue remodeling and repair [2,4,10]. The phenotypic response of microglia to anti-inflammatory cytokines including IL-10 is described with the term "deactivated". Microglia exhibit this deactivated phenotype in healthy conditions and may play a central role in maintenance of tissue homeostasis through communication with astrocytes and neurons. Several feedback mechanisms are described to attenuate inflammatory processes including induction of proteins that inhibit signal transduction pathways or anti-inflammatory cytokines (e.g. IL-10). All these actions allow microglia to serve as an immune surveillant in the CNS and they appear to be the main sensor of foreign signals recognized by PRRs. In response to this danger recognition, microglia secrete inflammatory mediators including TNF-α and IL-1β, which start the inflammatory cascade. Critical roles in establishing and maintaining inflammatory responses in neurodegenerative diseases are thus ascribed to microglial cells [4,11].

Neuroinflammation is related with many neurodegenerative diseases including AD, PD, ALS and MS. Increasing evidence suggests an active role of neuroinflammation in pathophysiology and disease progression as most neurodegenerative disorders are characterized by neuroinflammatory processes [4,12]. Specific for AD, the current hypothesis includes that activated microglia are protective in early stages of AD by promoting Aβ clearance but they become increasingly dysfunctional at later disease stages and consequently contribute to disease progression [12-18]. As the incidence of neurodegenerative disorders increases and treatment is in most cases only effective in the early stage of disease, diagnosis needs to be as early as possible. Because these neuropathologies are accompanied with neuroinflammation, detection of neuroinflammation is an interesting target for follow-up of disease progression and treatment. This highlights the importance of molecular (functional) imaging techniques, like PET, as they have the advantage of allowing detection of diseases in a much earlier stage than do structural imaging techniques.

B. Positron Emission Tomography Imaging

Molecular imaging can be defined as a multidisciplinary field that aims to integrate patient-specific and disease-specific molecular information with traditional anatomical imaging readouts. In the past, *in vivo* imaging methods have largely been based on imaging gross anatomy. As a consequence, disease or treatment effects were mostly detected as structural abnormalities or morphological changes (= structural imaging). PET and single photon emission computed tomography (SPECT) allow to visualize molecular interactions using specific radiolabeled probes (= functional imaging). The main advantage of functional imaging over structural imaging is its potential for early detection of disease. In most pathologies, functional discrepancies appear in an earlier stage of disease than do structural deviations. For this reason, especially PET is extremely useful for early disease diagnosis.

PET is an *in vivo* molecular imaging technology based on tracers that are labeled with positron-emitting radionuclides (table 1). The spatial and temporal distribution of the tracer can be visualized by a PET camera. Non-invasive molecular imaging using PET provides information about protein localization and density and organ function in general. Briefly, positron emitting radionuclides are unstable due to an excess of protons in their nucleus. As a result a proton is converted to a neutron and a positron which is ejected from the nucleus and travels a short distance (depending on its kinetic energy) and combines with an electron in the surrounding tissue to form a positronium. The distance the positron travels, is called the positron range and results in an inherent image blur. The positronium will annihilate, thereby converting the mass of the particle into electromagnetic energy namely two gamma ray photons of 511 keV which are emitted over an angle of 180°. This pair of gamma rays can be detected by a ring of detectors and detection of multiple coincident 511-keV gamma rays enables reconstruction of a 3D image representing the quantitative distribution of the radionuclide [19,20]. The most commonly used radionuclides in PET tracer development are carbon-11 and fluorine-18. These radionuclides are produced in a cyclotron, usually by proton bombardment of nitrogen-14 and oxygen-18, respectively. Carbon-11 decays to boron-11 by positron emission and has a half-life of 20.4 min. Fluorine-18 decays to oxygen-18 by positron emission and has a half-life of 109.8 min. The short half-life of carbon-11 enables multiple scans on the same day in the same subject with the same or a different tracer, however on-site production using a cyclotron combined with a fast and efficient chemical incorporation into precursors is required. The half-life of fluorine-18 on the other hand is long enough to allow for longer and more complicated radiosynthesis and for transport of fluorine-18 labeled tracers from the site of production to remote nuclear medicine departments not equipped with a cyclotron.

The ideal PET tracer should exhibit following characteristics: it should have a high affinity for the target, i.e. having an equilibrium dissociation constant (K_d) value in the subnanomolar to low nanomolar range. The affinity of the tracer for its target should be at least 5 to 10-fold higher than the target (receptor) expression (B_{max}). Also a high selectivity for the target is required, preferably 100-fold less affinity for any other binding site with the same expression level [21].

The blood-brain barrier (BBB) is a major hurdle in the development of drugs targeting the brain. Passive transfer across the BBB is promoted by low molecular mass (< 500 Da), a polar surface area (PSA) less than 80 $Å^2$, lack of a formal charge at physiological pH and a $logD_{7.4}$ (distribution coefficient at pH 7.4) in the approximate range 1-3. Large and hydrophilic molecules are therefore excluded from penetration or diffusion into the brain, except if a specific carrier for such a molecule exists. In addition, tracer uptake in the brain is influenced by efflux transporters like P-glycoproteins which are highly prevalent at the BBB. Substrates for P-glycoproteins are in general highly lipophilic, carry a positive charge at pH 7.4 and have multiple aromatic groups [21,22]. Highly lipophilic molecules usually also show a high non-specific binding to lipophilic membranes and proteins *in vivo*. The slow protein dissociation of tracers with high *in vivo* plasma protein binding hampers the brain uptake of these tracers as only the unbound fraction can cross the BBB. Moreover, highly lipophilic tracers complicate formulation for intravenous injection due to low solubility in water and adsorption of molecules on the surface of vials and syringes. After crossing the BBB, the ideal tracer should show low non-specific binding in the brain, reversible (allowing an equilibrium binding and kinetic modeling) and specific target binding, no toxicity and no metabolism in the brain or formation of lipophilic radiometabolites that cross the BBB. As a PET camera can not discriminate between different chemical forms of the positron emitting radionuclide, the presence of radiometabolites in the brain contaminates the specificity of the tracer signal in the CNS and hinders accurate quantification [21].

Nuclear imaging in general also has some limitations including patient exposure to ionising radiation, poor anatomical information and a low resolution compared to other molecular imaging modalities. The latter constraints are resolved by coupling functional imaging to structural imaging (= hybrid or fusion-imaging). This approach introduced magnetic resonance imaging (MRI) and computerized tomography (CT) fusion systems (PET-MRI/CT, SPECT-MRI/CT). In these fusion systems, the higher-resolution anatomical detail from MRI or CT compensates for the lower-resolution molecular information from PET or SPECT. The combination of the

Table 1. Radionuclides used in PET [23]

Radionuclide	Half-life production	Mode of decay (%)	$E_{\beta^+ max}$ (keV) max. range in H_2O (mm)	chemistry
^{11}C	20.4 min Cyclotron	β^+ (100 %)	960 keV 3.9 mm	Fast organic chemistry
^{13}N	9.97 min Cyclotron	β^+ (100 %)	1198 keV 5.1 mm	Fast organic chemistry
^{15}O	2.03 min Cyclotron	β^+ (100 %)	1732 keV 8.0 mm	Fast on-line gas phase chemistry
^{18}F	109.8 min Cyclotron	β^+ (97 %) EC (3 %)	634 keV 2.3 mm	Fast organic chemistry
^{64}Cu	12.7 h Cyclotron	β^+ (100 %)	653 keV 2.4 mm	Chelation chemistry
^{68}Ga	68 min Generator	β^+ (89 %) EC (11 %)	1899 keV 8.9 mm	Chelation chemistry
^{89}Zr	78.4 h Cyclotron	β^+ (100 %)	897 keV 3.6 mm	Chelation chemistry
^{124}I	4.17 d cyclotron	β^+ (23 %) EC (77 %)	1535 keV (50 %) 6.9 mm 2138 keV (50 %) 10.2 mm	Organic chemistry

two techniques will play an increasing role in clinical molecular imaging [24].

2. PET IMAGING OF NEUROINFLAMMATION

Neuroinflammation is expected to contribute to several human brain disorders, including cerebral ischemia, trauma, spinal cord injury, MS, acquired immune deficiency syndrome (AIDS) dementia, PD and AD. Although variations in glucose metabolism and cerebral blood flow have successfully been exploited to detect neuroinflammation using PET and SPECT, changes in these parameters lack specificity for neuroinflammation as they can be induced by other causes as well (e.g. hypercapnia increases cerebral blood flow). Several physiological parameters are altered during cerebral inflammation and these indicators are relatively specific for neuroinflammation and will be further discussed below, together with an overview of the reported PET tracers developed for these more specific neuroinflammatory targets.

A. Translocator Protein (TSPO)

The TSPO receptor, also called the peripheral benzodiazepine receptor (PBR), is one of the most studied biomarkers of neuroinflammation. The abbreviation TSPO has been taken over from the corresponding protein found in the outer mitochondrial membrane of bacteria, i.e. tryptophan-rich sensory protein (TspO). Two benzodiazepine receptors are expressed in humans. The central benzodiazepine receptor is coupled to the ɣ-aminobutyric acid A receptor ($GABA_AR$) and modulates GABA-regulated opening of Cl^- channels and inhibition of neuronal activity. The PBR receptor or TSPO receptor is an 18-kDa protein consisting of 169 amino acids. TSPO is part of a multimeric complex existing of the 32-kDa voltage-dependent anion channel (VDAC) and the 30-kDa adenine nucleotide carrier (ANC) located in the outer mitochondrial membrane of microglial cells [25,26]. A variety of physiological functions such as cell growth and proliferation, bile acid synthesis, calcium flow, chemotaxis and cellular immunity, heme biosynthesis, mitochondrial respiration, apoptosis and steroidogenesis are ascribed to TSPO. In addition, TSPO plays a crucial role in neurosteroidogenesis and more specifically in the transmembrane transport of cholesterol from the outer to the inner mitochondrial membrane, where the side chain cleavage by cytochrome p450 converts cholesterol into pregnenolone. Pregnenolone is an important precursor for cerebral steroids which play a crucial role in brain development and normal functioning during adulthood. Because of the correlation between TSPO activation and stimulation of neurosteroid synthesis, TSPO ligands are potential therapeutic agents for brain injury and inflammation. Under healthy circumstances, TSPO levels in the CNS are low. In response to brain inflammation, TSPO levels increase dramatically in glial cells as detected in several neurodegenerative diseases such as PD, ALS, HD and AD. Literature suggests that cytokines might play a role in increasing TSPO expression in various cell types. TSPO upregulation has also been detected in astrocytes. In contrast to microglia (early up-regulation after injury), astrocytes display a delayed, but more persistent induction of TSPO expression during astrocytosis which appears at later time points after the onset of brain injury [12,25,27,28].

Since the response of TSPO to injury is correlated with the degree of damage in neuroinflammation, TSPO has been identified as a promising biomarker for neuroinflammation and the number of PET radioligand candidates for TSPO has significantly increased in the last years (Fig. **1**). The most studied TSPO-radioligand is [^{11}C]PK11195, of which the R-enantiomer has an approximately 2-fold higher affinity for TSPO compared to the S-enantiomer. This isoquinoline derivative with nanomolar affinity for TSPO shows an increased binding in affected brain areas in neuroinflammatory

animal models as well as in humans. Although both microglia and astrocytes overexpress TSPO, a majority of the evidence suggests that [^{11}C]PK11195 binding in neurological diseases is increased in microglia with lower or less significant contributions from astrocytes. Until a few years ago it was the only PET tracer applied for imaging microglia activation in humans. Although [^{11}C]PK11195 has several limitations such as a high level of nonspecific binding and poor signal-to-noise ratios complicating its quantification, it is still used as a TSPO imaging agent by several research groups. For example zymosan-induced (focal white matter lesion) microglial activation and its response to minocycline was quantitatively imaged in rat brain using [^{11}C]PK11195 [29]. Folkersma *et al.* observed an increased cerebral uptake of this tracer ten days after traumatic brain injury in rats [30]. The widespread and prolonged increase in [^{11}C]PK11195 binding was also observed in patients until six months after traumatic brain injury [31]. Kumar *et al.* demonstrated an increased [^{11}C]PK11195 uptake with age in humans [32]. Increased [^{11}C]PK11195 binding was also observed in the cortex of patients with MS. The binding correlated with the degree of disability as assessed by the expanded disability status scale (EDSS) and the multiple sclerosis impact scale (MSIS) [33,34]. Other recent studies using [^{11}C]PK11195 have been performed by Gulyas *et al.* [35], Hughes *et al.* [36], Ren *et al.* [37], Rapic *et al.* [38], Garvey *et al.* [39], Boutin *et al.* [40] and Dickens *et al.* [41]. For an overview of *in vivo* PET imaging studies using [^{11}C]PK11195, the reader is referred to reviews of Venneti *et al.* [28], Chauveau *et al.* [42] and Owen and Matthews [43]. An overview of studies with other TSPO tracers is given in table 2. Note that for [^{11}C]CLINME and [^{18}F]GE-180 Ki values are given in table **2** as there are no data available in literature of binding affinity studies where these tracers are compared to PK11195 in the same assay.

Recently, Owen *et al.* [85,86] reported a TSPO polymorphism in man with a trimodal distribution in binding affinity (high-affinity binders, low-affinity binders and mixed affinity binders) for several TSPO ligands. Differences in affinity between high-affinity binders and low-affinity binders were approximately 50-fold with PBR28, approximately 17-fold with PBR06 and approximately 4-fold with DAA1106, DPA713 and PBR111. The consequence of this polymorphism is that knowledge of binding status is needed to correctly quantify TSPO expression using these PET ligands [85,86]. The reader should keep this in mind when looking at the affinities compared to PK11195 shown in table 2.

For a more detailed discussion on TSPO (PET) ligands, the reader is referred to some other reviews [42,43,87,88].

B. Cannabinoid 2 Receptor (CB_2R)

A second important target in neuroinflammation is the CB_2R. Two cannabinoid receptors have been described in literature: CB_1R and CB_2R. These receptors are $G_{i/o}$ protein coupled receptors, which upon activation inhibit adenylate cyclase and stimulate mitogen-activated protein kinases (MAPKs). Activation of CB_1R also leads to an inhibition of voltage-gated calcium channels and stimulation of inwardly rectifying potassium channels, whereas activation of CB_2R is coupled to an increased release of ceramide. Both receptors are involved in a release of nitric oxide and a subsequent activation of cyclic guanosine monophosphate (cGMP) levels [89]. The CB_2R is related to organs and tissues of the immune system with high expression in tonsils and spleen, whereas the CB_1R is mainly expressed in the central nervous system [90,91]. The CB_2R is upregulated in certain pathological conditions such as cancer, atherosclerosis, peripheral/central inflammation and several brain disorders [92-102]. Prolonged oral cannabinoid administration has been proposed to prevent neuroinflammation, result in lower Aβ levels and improve cognitive performance in Tg APP 2576 mice [103]. Microglial cells show very low CB_2R expression in basal conditions whereas in CNS pathologies the CB_2R expression is significantly increased. In experimental autoimmune encephalomyelitis (EAE), the expression of CB_2R is 10 times higher in activated microglia compared to basal levels [95,97].

The CB_2R is an interesting target for visualization of neuroinflammation as its expression in brain is very low in control conditions, but is upregulated in activated microglia. Evens *et al.* [104] synthesized and evaluated [^{11}C]methoxy-Sch225336 (Fig. **2**). Although this tracer displays low nanomolar affinity, its limited brain uptake makes this tracer unfavorable for imaging CB_2R expression in the brain [104]. Next, Evens *et al.* [105] synthesized carbon-11 and fluorine-18 labeled 2-oxoquinoline derivatives [^{11}C]NE40 and [^{18}F]oxoquinoline A (Fig. **2**) with nanomolar affinity for the human CB_2R. Both tracers were first evaluated in mice. Biodistribution studies showed uptake and washout of both tracers from brain whereas persistent accumulation was observed in the spleen. *In vitro* and *ex vivo* autoradiography confirmed the specificity of the CB_2R binding in the spleen. Both tracers were rapidly metabolized in plasma *in vivo*, whereas only a relatively small amount of radiometabolites was detected in brain [105]. [^{11}C]NE40 was then further evaluated in normal Wistar rats. The CB_2R specific spleen retention of [^{11}C]NE40 observed in the mice was even more pronounced in the rat biodistribution studies. *Ex vivo* autoradiography confirmed that the binding to rat spleen was specific for CB_2R. MicroPET studies in normal mouse, rat and rhesus monkey displayed relatively high brain uptake and moderately fast brain washout. No toxic (toxicity study in Wistar rats) or mutagenic (Ames test) effects were observed for NE40. Reversible binding to human CB_2R (hCB_2R) was confirmed by a microPET chase study with GW405833 (a nonstructurally related CB_2R partial agonist) in a rat model with local overexpression of hCB_2R [106,107]. Turkman *et al.* [108] synthesized and tested a library of new fluorinated 2-oxoquinoline CB_2R ligands with affinities in the nanomolar range [108]. *In vitro* autoradiography on tissues of CB_2R-expressing tumor bearing mice and *in vitro* binding assays with CB_2R expressing cell lysate showed that one of the fluorine-18 labeled oxoquinoline compounds, [^{18}F]oxoquinoline B (Fig. **2**), bound in a specific way to CB_2R. Unfortunately, its poor solubility hampered *in vivo* studies [109]. [^{11}C]A-836339 (Fig. **2**), developed by Horti *et al* [110], shows subnanomolar affinity for CB_2R and exhibits high specific CB_2R cerebral uptake in a LPS-induced mouse model of neuroinflammation and in a mouse model of AD [110]. GW405833, a known CB_2R partial agonist, was radiolabeled with [^{18}F]fluoroethyl bromide to introduce the fluorine-18 label via a fluoroethoxy chain. *In vitro* studies showed that [^{18}F]FE-GW405833 (Fig. **2**) has nanomolar affinity and selectivity for CB_2R. However, the presence of a large fraction of radiometabolites in brain arising from the loss and metabolism of the [^{18}F]fluoroethoxy chain, limits its use for imaging neuroinflammation [111]. The carbon-11 labeled derivative [^{11}C]GW405833 (Fig. **2**) on the other hand showed high BBB penetration, lower fraction of radiometabolites in brain, and reversible and specific CB_2R *in vivo* binding in an animal model with local overexpressing of CB_2R in the brain [106]. Other radiolabeled high affinity CB_2 ligands with no or limited *in vivo* evaluation will be discussed briefly. Triaryl ligands for the CB_2R with (sub)nanomolar affinity, synthesized by Fujinaga *et al.* [112], were labeled with carbon-11 and showed relatively high uptake in mouse brain [112]. Gao *et al.* [113] used quinolone derivatives as candidate PET radioligands for CB_2R imaging. Three compounds with nanomolar affinity and high selectivity for CB_2R were efficiently labeled with carbon-11 but unfortunately no *in vivo* studies were performed [113]. Rühl *et al.* [114] synthesized a number of N-aryl-oxa-diazolyl-propionamides with nanomolar affinity and selectivity for CB_2R over CB_1R. Imaging studies with the fluorine-18 labeled analogs are in progress [114]. Teodoro *et al.* [115] radiolabeled N-aryl-oxadiazolyl-propionamides successfully with fluorine-18 but the main radiometabolites were found to cross the BBB in mice

Table 2. Overview of studies with TSPO tracers

Tracer	Affinity (compared to PK11195)	Animal model/human pathology/experiments	Increased TSPO expression (yes or no)? Other information (in italics)?	References
[^{11}C]DAA1106	5-6 fold higher	Stereotactic LPS, 6-OHDA lesioned rat models	Yes	[44]
[^{11}C]PBR28	5-6 fold higher	Cerebral infaction rat	Yes	[45]
		Systemic LPS non-human primates	Yes	[46]
		Non-human primate, comparison with [^{11}C]PK11195	*Higher TSPO specific signal, less metabolism*	[47]
		Patients with temporal lobe epilepsy	Yes	[48]
		Radiation dosimetry, kinetic analysis in non-human primates and man	/	[49],[50],[51]
		Patients with Alzheimer's disease	Yes	[52]
		Patients with mild-to-moderate depression	No	[53]
[^{18}F]FEPPA	18 fold higher	Metabolite study in rat	*Few metabolites in brain*	[54]
		Quantitation in human brain; whole body distribution and radiation dosimetry in human	/	[55],[56]
		Healthy elderly individuals	No	[57]
[^{18}F]PBR28	2 fold higher	Stereotactic AMPA rat model	Yes	[58]
[^{18}F]fluoromethyl-PBR28	2 fold higher	Stereotactic lipopolysaccharide model	Yes	[59]
[^{18}F]FMDAA1106	5-6 fold higher	WT rats	*Specific binding*	[60]
		Non-human primate, metabolite study in mice	*[^{18}F)fluoride in plasma of mice, radioactivity in skull of non-human primate*	[61]
[^{18}F]FEDAA1106	8 fold higher	WT rat	*Specific binding*	[60]
		Non-human primate, metabolite study in mice	*High uptake in occipital corte, no metabolites in mouse brain*	[61]
		MS patients	No	[62]
[^{11}C]PBR01	11 fold higher	Non-human primate	*Pharmacokinetics*	[63],[64],[65]
[^{18}F]PBR06	11 fold higher	Mouse model of stroke	Yes	[66]
		Non-human primate	*Pharmacokinetics*	[63],[64],[65]
		Human	*Kinetic modeling, organ distribution*	[67],[68]
		Human	*Kinetic modeling, comparison of [^{18}F]PBR06 and [^{11}C]PBR28*	[69]
[^{18}F]DPA-714	1.5 fold higher	Stereotactic quinolinic acid rat model	Yes	[70]
		Stereotactic AMPA rat model	Yes	[71]
		Rat model of epilepsy, mouse model of stroke	*Yes*	[72]
		Rat model of cerebral ischemia	Yes	[40]
		Human	*Biodistribution, effective radiation dose of 17.2 μSv/MBq*	[73]
		Rat, baboon and human	*Metabolism and quantification*	[74]
		ALS patients	Yes	[75]
[^{11}C]DPA-713	2 fold higher	Stereotactic AMPA rat model	Yes	[71]
[^{11}C]CLINME	Ki of 8.52 nM*	Stereotactic AMPA rat model	Yes	[76],[77]

(Table 2) Contd.…

Tracer	Affinity (compared to PK11195)	Animal model/human pathology/experiments	Increased TSPO expression (yes or no)? Other information (in italics)?	References
[^{18}F]PBR111	2 fold higher	Stereotactic AMPA rat model	Yes	[77],[78]
		Post-kainic acid-induced status epilepticus rat model	Yes	[79]
		Non-human primate	*Radiation dosimetry*	[80]
		Healthy humans	*Quantitative assessment of TSPO expression*	[81]
[^{11}C]SSR180575	4 fold higher	Stereotactic AMPA rat model	Yes	[82,83]
[^{18}F]GE-180	Ki of 0.87 nM	Facial nerve axotomy rat model	Yes	[84]
		Stereotactic lipopolysaccharide rat model	Yes	[41]

*personal communication H. Boutin

[115]. Radiolabeling and *in vitro*/*in vivo* evaluation of N-(1-adamantyl)-8-methoxy-4-oxo-1-phenyl-1,4-dihydroquinoline-3-carboxamide is performed by Mu *et al.* [116]. This radiotracer showed promising *in vitro* characteristics but further *in vivo* research is needed [116]. A triazine derivative was radiolabeled with fluorine-18 by Hortala *et al.* [117]. This radiotracer has nanomolar affinity for the human CB_2R and was selective versus human CB_1R [117]. The reader is referred to the review of Evens and Bormans [21] for a complete overview of non-invasive imaging of the CB_2R using PET before 2010 [21].

C. Cyclooxygenase (COX)

COX is a intracellular key enzyme in the conversion of arachidonic acid to prostaglandins (PGs). Both lipid compounds are involved in several physiological and pathological processes, including (neuro)inflammation [118] indicating a key role of COX in the inflammatory cascade. Another indication for the role of COX in neuroinflammation is the fact that the use of nonsteroidal anti-inflammatory drugs (NSAIDs), which inhibit COX activity, is correlated with a reduced risk of developing AD later in life [119,120]. Several studies have confirmed these observations although some well-designed studies have found different results. Therefore Breitner *et al.* [121] analyzed the association of prior NSAID exposure with incident dementia and AD in an elderly community-based cohort. In contrast to the hypothesis that NSAIDs protect against dementia and AD, the authors observed an increased incidence of dementia and AD in heavy NSAID users [121]. Also in PD, neuroprotective characteristics have been ascribed to NSAIDs [122,123], although recent studies could not confirm this [124,125]. Two distinct COX isoforms, COX-1 and COX-2, have been characterized [126-128]. Along with COX-1 and COX-2, COX-3 is described in literature. COX-3 is a COX-1 splice variant inhibited by acetaminophen and other analgesic/antipyretic drugs [129]. COX-1 is constitutively expressed in most tissues and is considered responsible for homeostatic PG synthesis [130] whereas COX-2 is an enzyme inducible by inflammation. This led to the development of (selective) COX-2 inhibitors which do not disturb the physiological functions of COX-1-derived PGs. The expression of COX-2 is strongly elevated in brain by inflammatory stimuli and this overexpression is predominantly located in activated microglia and astrocytes [131]. Furthermore, increased COX-2 expression is implicated in a wide variety of cancers, including colorectal adenocarcinoma, breast and lung cancer [132-135]. COX-2 is also constitutively expressed in the CNS, where it has a pivotal role in synaptic activity, long-term synaptic plasticity [136,137] and in the neurovascular coupling during functional hyperemia [136]. In addition, studies have also indicated a previously unrecognized proinflammatory role of COX-1 in the pathophysiology of acute and chronic neurological disorders [138-142]. Overexpression of COX-1 and COX-2 has been reported in patients with ischemia, traumatic brain injury and in several neurodegenerative diseases such as AD, PD and ALS. These findings suggest that COX is a critical component in the neuroinflammatory processes associated with neurodegeneration [143-146].

In search of an appropriate PET tracer for COX-2 imaging some COX-2 inhibitors have been used as scaffold. One of the first developed PET tracers to image COX-2 was [^{11}C]arachidonic acid. However, PET studies showed incorporation of the tracer into phospholipids in the brain as expected since it is a building block for membrane lipids, making it unsuitable for COX-2 imaging [147-149]. Although favourable *in vitro* results were obtained with [^{18}F]SC58125, this tracer lacked specific binding *in vivo* [149,150]. Also for [^{18}F]desbromo-DuP-697, PET studies in pig showed absence of specific binding in the brain [149,151]. The [^{18}F]fluoromethyl analogue of valdecoxib, synthesized by Toyokuni *et al.* [152] was characterized by rapid defluorination *in vivo* in mice [152]. *In vivo* defluorination was also observed with [^{18}F]celecoxib derivative A (Fig. **3**) in rats. In baboons, however, defluorination was less pronounced and the distribution of the radioligand in baboon brain was consistent with the known distribution of COX-2. Nevertheless, because of the poor specific activity of [^{18}F]celecoxib an improved radiolabeling method should be developed [153]. Rofecoxib was labeled with carbon-11 by de Vries *et al.* (Fig. **3**) [154]. Although there was correlation between [^{11}C]rofecoxib uptake and COX-2 distribution in healthy rats, [^{11}C]rofecoxib could not detect COX-2 expression in two different rat models of inflammation [154]. Comley *et al.* [155] studied uptake and regional distribution of [^{11}C]rofecoxib in human brain and observed a heterogeneous distribution of the radiotracer [155]. Uddin *et al.* [156] evaluated a number of fluorinated derivatives of indomethacin and celecoxib as COX-2 PET imaging agents. A fluorinated derivative of celecoxib, [^{18}F]celecoxib derivative B (Fig. **3**), appeared to be the most promising lead. The radioligand showed sufficient metabolic and radiochemical stability to distribute to xenograft tumors and inflammatory lesions and exhibited highly selective uptake in inflammatory tissue and tumors compared to surrounding normal tissue in mice and rats [156]. Takashima-Hirano *et al.* [157] labeled several 2-arylpropionic acids and their esters with carbon-11. As was expected the 2-aryl[^{11}C]pro-pionic acids, the pharmacologically active forms, displayed low levels of brain uptake whereas the 2-aryl[^{11}C]propionic acid methyl esters

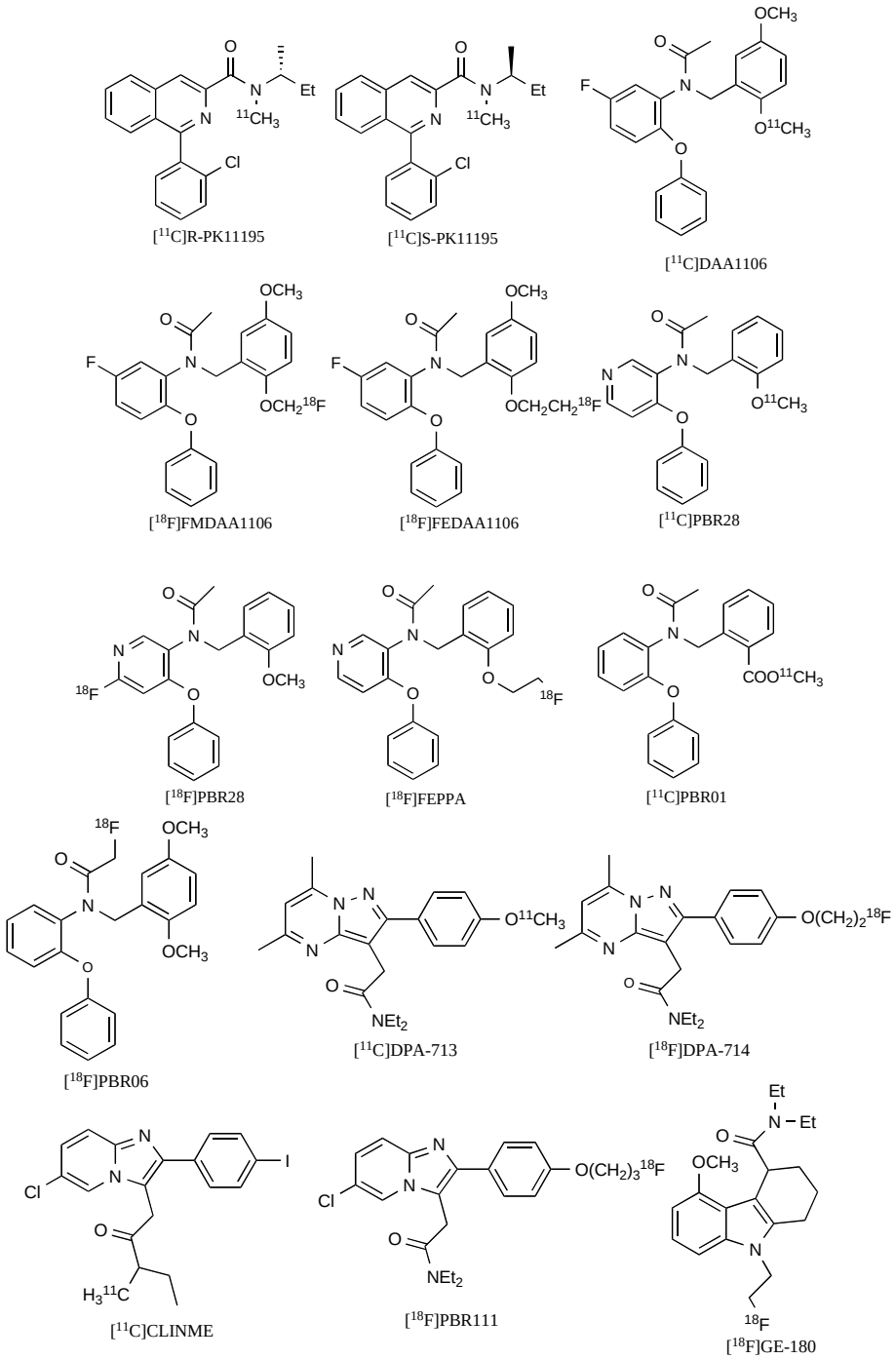

Fig. (1). Structure of TSPO PET tracers.

esters showed high BBB penetration. Radiometabolite analysis of [^{11}C]ketoprofen methyl ester in rat brain showed conversion into the pharmacologically active form [^{11}C]ketoprofen (Fig. **3**). [^{11}C]Naproxen methyl ester, [^{11}C]flurbiprofen methyl ester, [^{11}C]fenoprofen methyl ester, [^{11}C]ketoprofen methyl ester and [^{11}C]loxoprofen methyl ester all showed higher uptake into the lesioned hemisphere of an LPS-induced neuroinflammation rat model compared to the contralateral nontreated area. More than 90% of the proradiotracer was hydrolyzed after 5 min in rat brain. This first hydrolase activity step should be kept in mind when analyzing PET images. In order to determine the binding specificity of 2-aryl[^{11}C]propionic acid methyl esters as proradiotracer in the inflamed area, the authors performed blocking microPET and *ex vivo* autoradiography experiments with [^{11}C]ketoprofen methyl ester. Co-injection of the cold ketoprofen methyl ester resulted in a significant reduction of radioactivity in the area of LPS-induced inflammation. The authors conclude that this indicates that [^{11}C]ketoprofen binds specifically to COX-2 [157] but it is not clear whether they took into account the first step hydrolysis of the proradiotracer. Probably hydrolase activity is measured instead of COX-2 activity.

D. Matrix Metalloproteinase (MMP)

MMPs are secreted extracellular targets for imaging of neuroinflammation. As their name implies, MMPs are involved in turnover and degradation of the extracellular matrix. They belong to a family

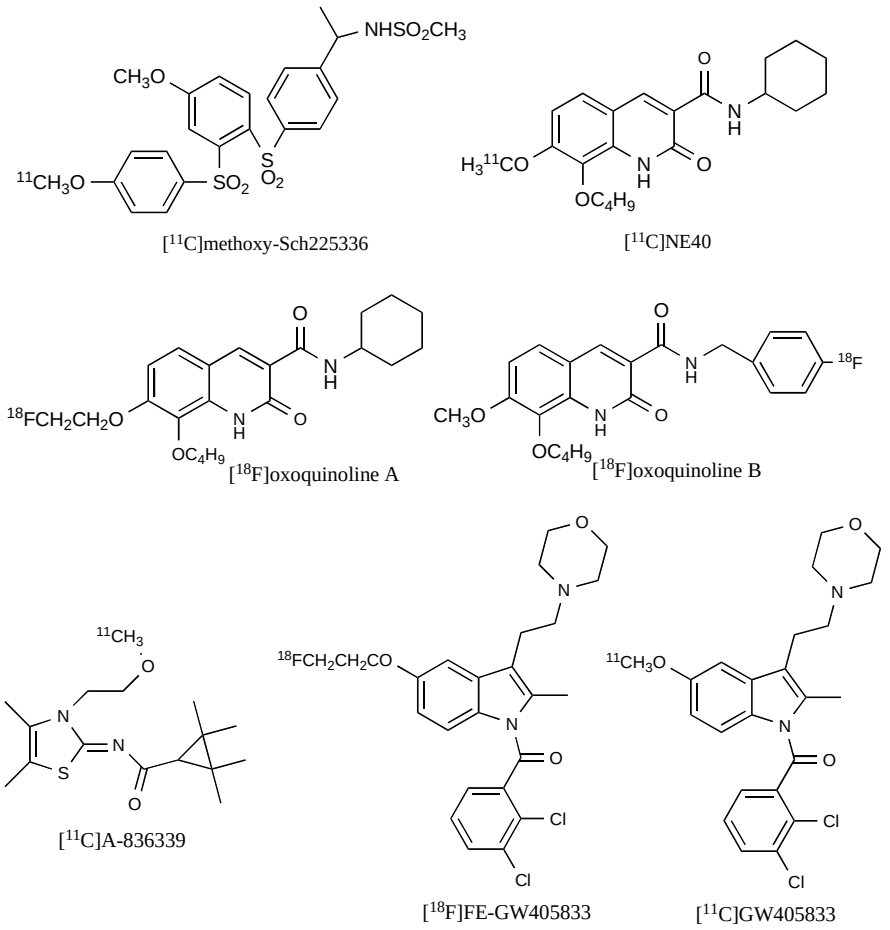

Fig. (2). CB_2R PET tracers.

of zinc- and calcium-dependent endopeptidases. Besides degradation of the extracellular matrix, MMPs act on pro-inflammatory cytokines, chemokines and other inflammation related proteins [158,159]. MMPs are synthesized as inactive zymogens and have a very low expression level in healthy tissues whereas elevated MMP expression has been found in disease processes like atherosclerosis, tumor cell metastasis and inflammation [158,160-162]. MMP activity is controled at four levels: gene expression, compartimentalization, zymogen activation and by endogenous tissue inhibitors of metalloproteinases (TIMPs) [158,163]. Vos *et al.* [164] showed expression of MMP-12 in phagocytotic macrophages in active MS lesions (human tissue) indicating a role for MMP-12 during demyelination in MS [164]. Nuttall *et al.* [165] activated human microglial cells with LPS resulting in a significant increase in mRNA levels of MMP-1, MMP-3, MMP-8, MMP-10 and MMP-12 [165]. Upregulation of MMP-12 expression was also observed in a mouse model of EAE with disease progression together with the expression of other inflammation related cytokines [166]. Crocker *et al.* [167] compared MMP expression profiles in cultures of astrocytes and microglia. Astrocytes extracted from mouse brain constitutively expressed MMP-11, MMP-14 and MMP-2 and showed induction of MMP-3 in response to IL-1β but did not respond to LPS. In contrast, microglia extracted from mouse brain constitutively expressed high levels of MMP-12 and showed strong induction of MMP-9 and MMP-14 in response to LPS [167]. Liu *et al.* [168] described MMP-12 as an inflammatory activating marker which is upregulated in mouse brain during normal aging. MMP-12 should facilitate recruitment of bone marrow-derived microglia into the brain which could be a mechanism to enhance aging-associated neuroinflammation [168]. These articles indicate that MMPs play an important role during (neuro)inflammation. Although overexpression of many MMPs in CNS pathology is correlated with detrimental effects, MMPs also have various roles in beneficial activities as in neurogenesis, axonal growth and myelinogenesis. Whether MMPs become beneficial or detrimental after nervous system injuries is determined by the stage of the CNS injury, the type of injury and the pathophysiology of the disorder. For more information on MMPs and their (beneficial/detrimental) role in CNS, the reader is referred to Yong *et al.* [169].

Two approaches are being used for imaging MMPs. One approach is based on use of radiolabeled peptides or proteins acting as matrix metalloproteinase inhibitors (MMPIs). Another approach is based on radiolabeled small molecular mass non-peptidyl MMPIs [163]. Wagner *et al.* [159] published an overview of the PET ligands developed for MMP visualization before 2006. Although the focus in this review is mainly on PET/SPECT imaging of MMPs during cancer and atherosclerosis, the lead structures shown could also be used as a template to develop radiotracers for imaging of neuroinflammation [159]. The *N*-sulfonyl amino acid hydroxamates CGS 25966 and CGS 27023A (Fig. **4**) are broad-spectrum inhibitors of MMP-1, MMP-2, MMP-3 and MMP-9 in the nanomolar range and most radiolabeled MMPIs have been designed based on these lead structures [159]. Fluorine-18 labeled derivatives of CGS 27023A and CGS 25966, [^{18}F]CGS 27023 A 1 and [^{18}F]CGS 25966 1 (Fig. **4**), were synthesized and the non-radioactive compounds displayed IC_{50} values in the low nanomolar range. Biodistribution studies of both tracers in WT mice did not show tissue specific accumulation. The authors suggest that this low uptake in normal mice could be an advantage in studying activated and dysregulated MMPs but validation of the tracers in animal models of

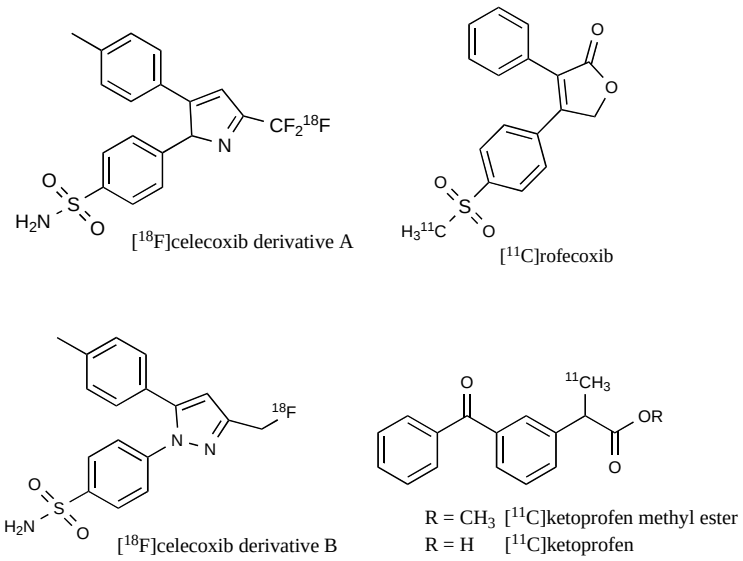

Fig. (3). COX-2 PET tracers.

neuroinflammation has not been reported [163,170]. Another [^{18}F]-labeled derivative of CGS 27023A ([^{18}F]CGS 27023 A 2, Fig. **4**) was also developed by Wagner *et al.* [163]. This compound showed IC_{50}-values in the nanomolar and subnanomolar range for MMP-2, MMP-8, MMP-9 and MMP-13. Initial small-animal PET *in vivo* studies in WT mice did not show any unfavourable aspecific tracer accumulation nor accumulation of free [^{18}F]fluoride in bone [163]. Breyholz *et al*. [171] designed barbiturate-based radiotracers for non-invasive imaging of MMPs. These pyrimidine-2,4,6-triones of which the structure is based on RO 28-2653 (Fig. **4**) exhibit specific activity for subgroups of secreted MMPs and have higher metabolic stability compared to hydroxamic acid-based MMP inhibitors, such as CGS 27023A. Biodistribution studies in WT mice of a fluorine-18 labeled derivative of RO 28-2653 ([^{18}F]RO 28-2653 derivative 1, Fig. **4**) with nanomolar IC_{50} values for MMP-2 and MMP-9 showed no tissue specific accumulation [171]. Schrigten *et al.* [172] continued the exploration of the barbiturate-based MMPIs and presented the synthesis and *in vitro* characterization of a new series of fluorinated pyrimidine-2,4,6-trione-based MMPIs. One of these MMPI, [^{18}F]RO 28-2653 derivative 2 (Fig. **4**), was successfully radiolabeled with fluorine-18 with high radiochemical yield and showed high *in vitro* stability. The IC_{50} -values for MMP-2 and MMP-9 were in the higher nanomolar range and the logD was 0.78 ± 0.02 which makes it a suitable PET tracer to image peripheral MMP expression but unsuitable for MMP imaging in the brain. In a next step preclinical PET/CT studies will be performed in animal models with known MMP up-regulation [172]. Recently, a fluorine-18 labeled triazole-substituted hydroxamate (Fig. **4**) with nanomolar IC_{50} values (0.006 - 107 nM) for MMP-2, MMP-8, MMP-9 and MMP-13 was reported by Hugenberg *et al.* [173]. The tracer showed high stability *in vitro* in mouse and human plasma. *In vivo* one polar radiometabolite was detected at 30 min post tracer injection. Biodistribution was studied *in vivo* with a microPET experiment in WT mice showing fast plasma clearance and absence of aspecific binding and defluorination. The tracer will be further evaluated in murine disease models with upregulated levels of activated MMPs [173]. Most compounds displayed in (Fig. **4**) are hydrophilic and this means difficult BBB penetration. Upon evaluation of these compounds in animal models of neuroinflammation, high brain uptake could be due to BBB damage.

E. Monoamine Oxidase-B (MAO-B)

Although this review mainly covers targets that are localized in microglia, astrocytes also express some proteins during inflammation which could be imaged by PET such as MAO-B. MAOs catalyze oxidative deamination of neurotransmitters and thus regulate their availability and physiological activity. Consequently, they are an important target for therapeutic drugs. More specifically, MAO-B inhibitors such as deprenyl are used to treat PD as they increase dopamine concentration in brain by inhibiting breakdown of dopamine. MAO-B is of special interest in imaging neuroinflammation because the MAO-B enzyme is upregulated in reactive astrocytes during neuroinflammation [35]. Several PET tracers have been proposed with structures derived from known MAO-B-inhibitors.

Carbon-11 labeled L-deprenyl (Fig. **5**) has been successfully used as a PET radioligand to image increased MAO-B activity in CNS diseases with neuroinflammation including pituitary adenoma [174], PD [175], focal epilepsy [176,177], traumatic brain injury [178], ALS [179] and AD [35,180]. Saba *et al*. [181] characterized [^{11}C]SL-25.1188 (Fig. **5**) in baboons for *in vivo* visualization of MAO-B using PET. The radioligand displayed high brain uptake, reversible binding and very slow plasma metabolism [181]. A carbon-11 labeled phenylmethanamine (Fig. **5**) was evaluated by Vasdev *et al.* [182] in WT rats and showed relatively high brain uptake that reflected regional MAO-B density in the brain and displayed moderate dose-dependent blocking with L-deprenyl. However, the signal-to-noise ratio was too low for further *in vivo* imaging studies [182]. [^{18}F]Fluorodeprenyl (Fig. **5**), developed by Nag *et al.* [183,184], accumulated in areas of the monkey brain known to express MAO-B. Pretreatment with L-deprenyl blocked the *in vivo* binding of [^{18}F]fluorodeprenyl whereas no significant effect on binding was observed after pretreatment with the MAO-A inhibitor clorgyline, demonstrating the selectivity for MAO-B [183,184]. The same research group labeled rasagiline with fluorine-18. This tracer has nanomolar *in vitro* binding affinity for MAO-B. [^{18}F]Fluororasagiline (Fig. **5**) exhibited high specificity for MAO-B in post-mortem human brain autoradiography. A PET imaging study in monkey showed high brain accumulation in known MAO-B rich regions. However, this accumulation in brain continued throughout the PET scan, which might indicate formation of a BBB penetrating radiometabolite complicating reliable quantification. Synthesis of a more stable radioligand is in progress [185]. Nag *et al.* [186] also radiolabeled propargylamines with fluorine-18. (*S*)-1-[^{18}F]fluoro-*N*,4-dimethyl-*N*-(prop-2-ynyl)pentan-2-amine (Fig. **5**) was selected for further investigation because of its favourable affinity and selectivity for MAO-B. High specific binding to regions with high MAO-B activity was observed in post-mortem human

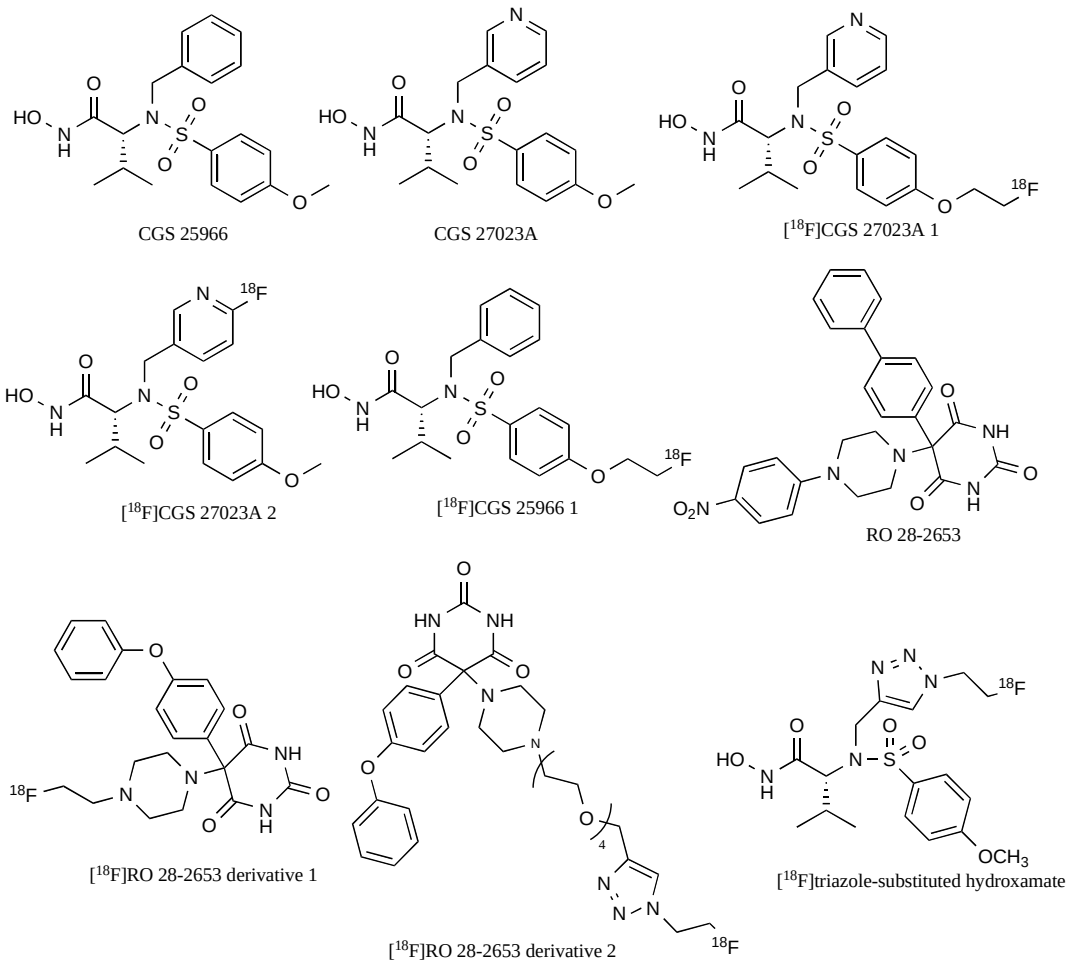

Fig. (4). MMP inhibitors and PET tracers.

brain autoradiography and *in vivo* PET studies in a cynomolgus monkey demonstrated high brain uptake and accumulation in known MAO-B rich regions [186].

F. P2X$_7$ Receptor (P2X$_7$R)

The P2X$_7$R appears to play an important role in cerebral inflammation and neurodegeneration and could be an interesting target for visualization of neuroinflammatory processes. The P2X$_7$R selectively expressed on cells of hematopoietic lineage including mast cells, lymphocytes, erythrocytes, fibroblasts, peripheral macrophages, epidermal Langerhans cells and within the nervous system on microglia, belongs to the family of purinergic ATP (adenosine-5'-triphosphate) binding receptors and has been reported to play a main role in cell-to-cell communication, cell proliferation, cytokine release and cell death [187,188]. These purinergic P2 receptors are categorized into two major families: the P2X ionotropic receptors (ATP-gated ion channels) and the P2Y metabotropic receptors (G protein-coupled receptors). In response to extracellular ATP, P2X$_7$R functions as an ion channel and is permeable to small cations such as Ca^{2+}, K^+ and Na^+. Prolonged activation of P2X$_7$R causes formation of a reversible plasma membrane pore permeable to molecules as large as 900 Da [188-190]. ATP is the only known endogenous activator of P2X$_7$R. Under physiological circumstances, extracellular ATP concentrations are low. On the contrary, intracellular ATP concentrations are in the millimolar range. Activated immune cells, macrophages, microglia, platelets and dying cells may release high amounts of ATP into the pericellular space, explaining the high extracellular ATP concentration during inflammation. In addition, proinflammatory cytokines induce upregulation of P2X$_7$R expression and increase its sensitivity to ATP [188]. Upregulation of P2X$_7$R has been demonstrated in several animal models such as the AD, HD and a prion disease animal model. More specifically for the AD model, Aβ triggers ATP release, increases intracellular Ca^{2+}, IL-1β secretion and generation of superoxide and plasma membrane permeabilization in microglia from WT but not in P2X$_7$R-deleted mice [189,191,192]. Recently, Diaz-Hernandez *et al.* [193] demonstrated that *in vivo* P2X$_7$R inhibition reduces Aβ plaques in AD through GSK3β and secretases [193]. This suggests that P2X$_7$R upregulation is correlated with activation of microglia and thus with the inflammatory response leading to progression of neuronal loss in AD. Suppression of the receptor attenuates the toxic effects of P2X$_7$R activation and plays a key role in pain modulation [188,194]. These facts make P2X$_7$R an interesting therapeutic target as well as a biomarker for neuroinflammation and for neurodegenerative disorders [189].

A number of P2X$_7$R antagonists including KN-62, PPADS, oxidized ATP and Brilliant Blue G have been developed in the past decade [195]. These antagonists however have a differential affinity for the human versus rodent P2X$_7$R limiting their usefulness as an *in vivo* tool to examine the P2X$_7$R expression in rat models of neuroinflammation. Recently, novel series of P2X$_7$R antagonists have been introduced: adamantane amides (f.e. A-847227 and GSK314181A), cubyl amides, substituted tri/tetrazoles (f.e. A-438079) and cyanoguanidines (f.e. A-740003 and A-804598) (Fig. **6**) [190,194,196-203]. Compared to the previous antagonists, these novel series show enhanced potency and selectivity as antagonists at both the rat and the human P2X$_7$R [195,204,205]. Besides the antagonists mentioned above, several other scaffolds have been

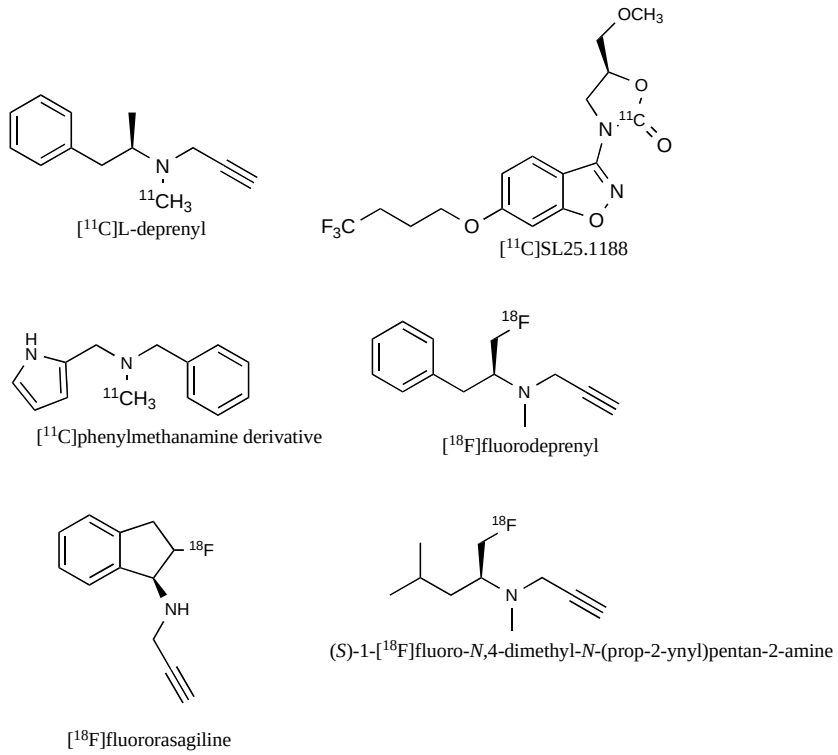

Fig. (5). MAO-B PET tracers.

used and optimized in structure-activity relationship (SAR) studies. Beswick *et al.* [206] developed a novel series of (1*H*-pyrazol-4-yl)acetamide $P2X_7$ antagonists with good *in vitro* potency, selectivity and pharmacokinetic properties [206]. Several other SAR studies have been performed by GlaxoSmithKline [207-209]. Also Pfizer, Merck Research Laboratories, Janssen Research and Development and other research groups performed SAR studies [210-217]. Comprehensive reviews on $P2X_7R$ antagonists and their therapeutic efficacy/use have been published by Donnelly-Roberts and Jarvis [195], Gunosewoyo *et al.* [204] Carroll *et al.* [201], Guile *et al.* [218], Gunosewoyo and Kassiou [219]. At this moment, no validated PET tracer to visualize $P2X_7R$ upregulation has been reported. Therefore it could be interesting to radiolabel these high-affinity $P2X_7R$-antagonists and evaluate them as potential neuroinflammation markers.

G. Histamine 4 Receptor (H_4R)

Histamine (Fig. **7**) is an endogenous short-acting amine formed from the basic amino acid histidine. Histamine exerts a wide range of biological effects through binding to four G protein-coupled receptors (GPCRs) and is known as a mediator in several (patho)physiological conditions. Unfortunately, less is known about its function in the brain. H_1 and H_2 receptors (H_1R and H_2R) are widely distributed and their function includes immunomodulation and gastric acid secretion, respectively [220,221]. The H_3 receptor (H_3R) is predominantly expressed in neurons and modulates neurotransmission [222,223]. The H_4R is the most recently discovered histamine receptor. It is prominently expressed in cells and tissues of the immune system and modulates the immune system [224,225]. All four GPCRs have been subject of intensive research and drugs acting on the histaminergic system have been developed. H_1R and H_2R antagonists are used to treat allergy and gastrointestinal disorders, respectively. H_3R antagonists could be used in treatment of dementias, obesity psychotic and sleep disorders. Nowadays, therapeutic exploitation of the H_4R in inflammation and cancer is of great interest [225]. The immunomodulation in cytokine production and the presence of H_4R in the immune system imply that the H_4R is involved in inflammatory processes as asthma, allergic disorders, autoimmune diseases and thus could be an interesting imaging target to visualize neuroinflammation. Interesting lead structures to synthesise H_4R PET ligands can be found in literature. Leurs *et al.* [224] describe several H_4R ligands with nanomolar affinity such as JNJ7777120, VUF10558 and A-943931 (Fig. **7**). These molecules could be interesting to be labeled with carbon-11 or fluorine-18 [224]. Other H_4R ligands have been developed by Strakhova *et al.* [226], Sander *et al.* [227], Savall *et al.* [228], Mowbray *et al.* [229] and Lane *et al.* [230] and are also interesting for labeling with carbon-11 or fluorine-18. Two of the mentioned lead structures, JNJ7777120 and VUF10558, were radiolabeled with carbon-11 and currently, [^{11}C]JNJ7777120 is being evaluated *in vivo* [231].

3. CONCLUSION

As the incidence of neurodegenerative disorders increases and treatment is in most cases only effective in the early stage of disease, diagnosis needs to be as early as possible. Since these neuropathologies are accompanied with neuroinflammation, detection of neuroinflammation is an interesting target for diagnosis and follow-up of disease progression and treatment.

Various targets are upregulated during neuroinflammatory processes and in neuropathologies. For each of these inflammation related targets, several PET tracers have been developed, evaluated and optimized. However, selecting the most reliable target to image neuroinflammation is difficult since interspecies differences in expression levels and protein sequence exist. In addition, the various animal disease models used to evaluate these tracers display different expression patterns of the upregulated proteins. It would be interesting to know which target in which disease is most prominently upregulated, this in order to correctly evaluate the degree of cerebral inflammation. Furthermore, since the activated microglia cells overexpress several inflammation related proteins, it is difficult to study the specificity of the tracer binding in these general inflammation models. Blocking all other known upregulated binding sites is necessary to determine the specificity. Development of

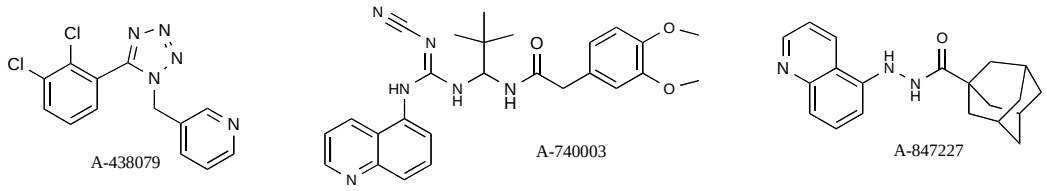

Fig. (6). $P2X_7R$ antagonists.

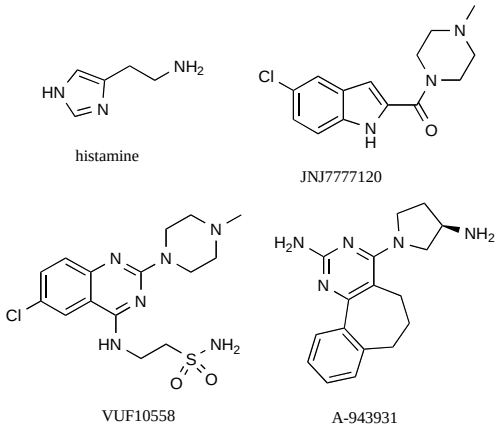

Fig. (7). H_4R ligands.

animal models with local overexpression of a specific neuroinflammatory target protein would be more straightforward. In case large interspecies differences with regard to affinity of ligands exists, the animal models should preferably overexpress human target proteins. Another important issue to bear in mind is the possible damage to the BBB in certain animal models. Before concluding there is an increased expression of the inflammation related target, it should be verified wether BBB integrity is not affected (for example with magnetic resonance imaging).

Up till now TSPO is the most studied target to image neuroinflammation. However, recent findings suggest a TSPO polymorphism resulting in differences in binding affinity of PET radioligands for TSPO. As a consequence, knowledge of the binding status of the individual patient is required to correctly interpret the PET images.

The development of radiotracers for imaging TSPO, CB_2 and COX continues but recently also new interesting targets have appeared. This, together with the search for better animal models of neuroinflammation makes the search for an ideal biomarker of neuroinflammation continuous and fascinating.

CONFLICT OF INTEREST

The authors confirm that this article content has no conflict of interest.

ACKNOWLEDGEMENTS

Dieter Ory is a fellow of the Research Foundation Flanders (FWO). The compilation of this literature review has been made possible by the funding from the European Union's Seventh Framework Programme (FP7/2007-2013) under grant agreement n° HEALTH-F2-2011-278850 (INMiND) and by the *In vivo* Molecular Imaging Research group K.U.Leuven (IMIR).

REFERENCES

[1] Graeber MB, Li W, Rodriguez ML. Role of microglia in CNS inflammation. FEBS Lett 2011; 585: 3798-805.

[2] Jacobs AH, Tavitian B. Noninvasive molecular imaging of neuroinflammation. J Cereb Blood Flow Metab 2012; 32: 1393-415.

[3] Chen GY, Nuñez G. Sterile inflammation: sensing and reacting to damage. Nat Rev Immunol 2010; 10: 826-37.

[4] Glass CK, Saijo K, Winner B, Marchetto MC, Gage FH. Mechanisms underlying inflammation in neurodegeneration. Cell 2010; 140: 918-34.

[5] Chen X, Walker DG, Schmidt AM, Arancio O, Lue LF, Yan S Du. RAGE: a potential target for Abeta-mediated cellular perturbation in Alzheimer's disease. Curr Mol Med 2007; 7: 735-42.

[6] Fang F, Lue LF, Yan S, *et al.* RAGE-dependent signaling in microglia contributes to neuroinflammation, Abeta accumulation, and impaired learning/memory in a mouse model of Alzheimer's disease. FASEB J 2010; 24: 1043-55.

[7] Shaw PJ, Lamkanfi M, Kanneganti TD. NOD-like receptor (NLR) signaling beyond the inflammasome. Eur J Immunol 2010; 40: 624-7.

[8] Di Virgilio F, Ceruti S, Bramanti P, Abbracchio MP. Purinergic signalling in inflammation of the central nervous system. Trends Neurosci 2009; 32: 79-87.

[9] Husemann J, Loike JD, Anankov R, Febbraio M, Silverstein SC. Scavenger receptors in neurobiology and neuropathology: their role on microglia and other cells of the nervous system. Glia 2002; 40: 195-205.

[10] Czeh M, Gressens P, Kaindl AM. The yin and yang of microglia. Dev Neurosci 2011; 33: 199-209.

[11] Garden GA, Möller T. Microglia biology in health and disease. J Neuroimmune Pharmacol 2006; 1: 127-37.

[12] Venneti S, Wiley CA, Kofler J. Imaging microglial activation during neuroinflammation and Alzheimer's disease. J Neuroimmune Pharmacol 2009; 4: 227-43.

[13] Blasko I, Stampfer-Kountchev M, Robatscher P, Veerhuis R, Eikelenboom P, Grubeck-Loebenstein B. How chronic inflammation can affect the brain and support the development of Alzheimer's disease in old age: the role of microglia and astrocytes. Aging Cell 2004; 3: 169-76.

[14] Arnaud L, Robakis NK, Figueiredo-Pereira ME. It may take inflammation, phosphorylation and ubiquitination to "tangle" in Alzheimer's disease. Neurodegener Dis 2006; 3: 313-9.

[15] Hickman SE, Allison EK, El Khoury J. Microglial dysfunction and defective beta-amyloid clearance pathways in aging Alzheimer's disease mice. J Neurosci 2008; 28: 8354-60.

[16] Rojo LE, Fernández JA, Maccioni AA, Jimenez JM, Maccioni RB. Neuroinflammation: implications for the pathogenesis and

molecular diagnosis of Alzheimer's disease. Arch Med Res 2008; 39: 1-16.

[17] Maccioni RB, Rojo LE, Fernández JA, Kuljis RO. The role of neuroimmunomodulation in Alzheimer's disease. Ann N Y Acad Sci 2009; 1153: 240-6.

[18] Eikelenboom P, van Exel E, Hoozemans JJM, Veerhuis R, Rozemuller AJM, van Gool WA. Neuroinflammation - an early event in both the history and pathogenesis of Alzheimer's disease. Neurodegener Dis 2010; 7: 38-41.

[19] Green M V, Seidel J, Vaquero JJ, Jagoda E, Lee I, Eckelman WC. High resolution PET, SPECT and projection imaging in small animals. Comput Med Imaging Graph 25: 79-86.

[20] Miller PW, Long NJ, Vilar R, Gee AD. Synthesis of 11C, 18F, 15O, and 13N radiolabels for positron emission tomography. Angew Chem Int Ed Engl 2008; 47: 8998-9033.

[21] Evens N, Bormans GM. Non-invasive imaging of the type 2 cannabinoid receptor, focus on positron emission tomography. Curr Top Med Chem 2010; 10: 1527-43.

[22] Pike VW. PET radiotracers: crossing the blood-brain barrier and surviving metabolism. Trends Pharmacol Sci 2009; 30: 431-40.

[23] Serdons K, Verbruggen A, Bormans GM. Developing new molecular imaging probes for PET. Methods 2009; 48: 104-11.

[24] Jaffer FA, Weissleder R. Molecular imaging in the clinical arena. JAMA 2005; 293: 855-62.

[25] Chen M-K, Guilarte TR. Translocator protein 18 kDa (TSPO): molecular sensor of brain injury and repair. Pharmacol Ther 2008; 118: 1-17.

[26] Cosenza-Nashat M, Zhao M-L, Suh H-S, *et al*. Expression of the translocator protein of 18 kDa by microglia, macrophages and astrocytes based on immunohistochemical localization in abnormal human brain. Neuropathol Appl Neurobiol 2009; 35: 306-28.

[27] Mattner F, Katsifis A, Staykova M, Ballantyne P, Willenborg DO. Evaluation of a radiolabelled peripheral benzodiazepine receptor ligand in the central nervous system inflammation of experimental autoimmune encephalomyelitis: a possible probe for imaging multiple sclerosis. Eur J Nucl Med Mol Imaging 2005; 32: 557-63.

[28] Venneti S, Lopresti BJ, Wiley CA. The peripheral benzodiazepine receptor (Translocator protein 18kDa) in microglia: from pathology to imaging. Prog Neurobiol 2006; 80: 308-22.

[29] Converse AK, Larsen EC, Engle JW, Barnhart TE, Nickles RJ, Duncan ID. 11C-(R)-PK11195 PET imaging of microglial activation and response to minocycline in zymosan-treated rats. J Nucl Med 2011; 52: 257-62.

[30] Folkersma H, Foster Dingley JC, van Berckel BNM, *et al.* Increased cerebral (R)-[(11)C]PK11195 uptake and glutamate release in a rat model of traumatic brain injury: a longitudinal pilot study. J Neuroinflammation 2011; 8: 67.

[31] Folkersma H, Boellaard R, Yaqub M, *et al.* Widespread and prolonged increase in (R)-(11)C-PK11195 binding after traumatic brain injury. J Nucl Med 2011; 52: 1235-9.

[32] Kumar A, Muzik O, Shandal V, Chugani D, Chakraborty P, Chugani HT. Evaluation of age-related changes in translocator protein (TSPO) in human brain using (11)C-[R]-PK11195 PET. J Neuroinflammation 2012; 9: 232.

[33] Politis M, Giannetti P, Su P, *et al.* Increased PK11195 PET binding in the cortex of patients with MS correlates with disability. Neurology 2012; 79: 523-30.

[34] Politis M, Su P, Piccini P. Imaging of microglia in patients with neurodegenerative disorders. Front Pharmacol 2012; 3: 96.

[35] Gulyás B, Pavlova E, Kása P, *et al.* Activated MAO-B in the brain of Alzheimer patients, demonstrated by [11C]-L-deprenyl using whole hemisphere autoradiography. Neurochem Int 2011; 58: 60-8.

[36] Hughes JL, Jones PS, Beech JS, *et al*. A microPET study of the regional distribution of [11C]-PK11195 binding following temporary focal cerebral ischemia in the rat. Correlation with post mortem mapping of microglia activation. Neuroimage 2012; 59: 2007-16.

[37] Ren W, Muzik O, Jackson N, *et al.* Differentiation of septic and aseptic loosening by PET with both 11C-PK11195 and 18F-FDG in rat models. Nucl Med Commun 2012; 33: 747-56.

[38] Rapic S, Backes H, Viel T, *et al*. Imaging microglial activation and glucose consumption in a mouse model of Alzheimer's disease. Neurobiol Aging 2013; 34: 351-4.

[39] Garvey LJ, Pavese N, Politis M, *et al.* Increased microglia activation in neurologically asymptomatic HIV-infected patients receiving effective ART; An 11C-PK11195 PET study. AIDS 2013;

[40] Boutin H, Prenant C, Maroy R, *et al.* [18F]DPA-714: direct comparison with [11C]PK11195 in a model of cerebral ischemia in rats. PLoS One 2013; 8: e56441.

[41] Dickens AM, Vainio S, Marjamäki P, *et al.* Detection of Microglial Activation in an Acute Model of Neuroinflammation Using PET and Radiotracers 11C-(R)-PK11195 and 18F-GE-180. J Nucl Med 2014;

[42] Chauveau F, Boutin H, Van Camp N, Dollé F, Tavitian B. Nuclear imaging of neuroinflammation: a comprehensive review of [11C]PK11195 challengers. Eur J Nucl Med Mol Imaging 2008; 35: 2304-19.

[43] Owen DRJ, Matthews PM. Imaging brain microglial activation using positron emission tomography and translocator protein-specific radioligands. Int Rev Neurobiol 2011; 101: 19-39.

[44] Venneti S, Lopresti BJ, Wang G, *et al.* A comparison of the high-affinity peripheral benzodiazepine receptor ligands DAA1106 and (R)-PK11195 in rat models of neuroinflammation: implications for PET imaging of microglial activation. J Neurochem 2007; 102: 2118-31.

[45] Imaizumi M, Kim H-J, Zoghbi SS, *et al.* PET imaging with [11C]PBR28 can localize and quantify upregulated peripheral benzodiazepine receptors associated with cerebral ischemia in rat. Neurosci Lett 2007; 411: 200-5.

[46] Hannestad J, Gallezot J-D, Schafbauer T, *et al.* Endotoxin-induced systemic inflammation activates microglia: [^{11}C]PBR28 positron emission tomography in nonhuman primates. Neuroimage 2012; 63: 232-9.

[47] Briard E, Zoghbi SS, Imaizumi M, *et al*. Synthesis and evaluation in monkey of two sensitive 11C-labeled aryloxyanilide ligands for imaging brain peripheral benzodiazepine receptors *in vivo*. J Med Chem 2008; 51: 17-30.

[48] Hirvonen J, Kreisl WC, Fujita M, *et al.* Increased *in vivo* expression of an inflammatory marker in temporal lobe epilepsy. J Nucl Med 2012; 53: 234-40.

[49] Brown AK, Fujita M, Fujimura Y, *et al.* Radiation dosimetry and biodistribution in monkey and man of 11C-PBR28: a PET radioligand to image inflammation. J Nucl Med 2007; 48: 2072-9.

[50] Fujita M, Imaizumi M, Zoghbi SS, *et al.* Kinetic analysis in healthy humans of a novel positron emission tomography radioligand to image the peripheral benzodiazepine receptor, a potential biomarker for inflammation. Neuroimage 2008; 40: 43-52.

[51] Imaizumi M, Briard E, Zoghbi SS, *et al.* Brain and whole-body imaging in nonhuman primates of [11C]PBR28, a promising PET radioligand for peripheral benzodiazepine receptors. Neuroimage 2008; 39: 1289-98.

[52] Kreisl WC, Lyoo CH, McGwier M, *et al. In vivo* radioligand binding to translocator protein correlates with severity of Alzheimer's disease. Brain 2013; 136: 2228-38.

[53] Hannestad J, DellaGioia N, Gallezot J-D, *et al.* The neuroinflammation marker translocator protein is not elevated in individuals with mild-to-moderate depression: a [^{11}C]PBR28 PET study. Brain Behav Immun 2013; 33: 131-8.

[54] Wilson AA, Garcia A, Parkes J, *et al.* Radiosynthesis and initial evaluation of [18F]-FEPPA for PET imaging of peripheral benzodiazepine receptors. Nucl Med Biol 2008; 35: 305-14.

[55] Rusjan PM, Wilson AA, Bloomfield PM, *et al.* Quantitation of translocator protein binding in human brain with the novel radioligand [18F]-FEPPA and positron emission tomography. J Cereb Blood Flow Metab 2011; 31: 1807-16.

[56] Mizrahi R, Rusjan PM, Vitcu I, *et al.* Whole body biodistribution and radiation dosimetry in humans of a new PET ligand, [(18)F]-FEPPA, to image translocator protein (18 kDa). Mol Imaging Biol 2013; 15: 353-9.

[57] Suridjan I, Rusjan PM, Voineskos AN, *et al*. Neuroinflammation in healthy aging: A PET study using a novel Translocator Protein 18kDa (TSPO) radioligand, [(18)F]-FEPPA. Neuroimage 2013; 84C: 868-75.

[58] Damont A, Boisgard R, Kuhnast B, *et al.* Synthesis of 6-[^{18}F]fluoro-PBR28, a novel radiotracer for imaging the TSPO 18 kDa with PET. Bioorg Med Chem Lett 2011; 21: 4819-22.

[59] Moon BS, Kim BS, Park C, *et al*. [(18)F]Fluoromethyl-PBR28 as a Potential Radiotracer for TSPO: Preclinical Comparison with [(11)C]PBR28 in a Rat Model of Neuroinflammation. Bioconjug Chem 2014;

[60] Zhang M-R, Kida T, Noguchi J, *et al.* [(11)C]DAA1106: radiosynthesis and *in vivo* binding to peripheral benzodiazepine receptors in mouse brain. Nucl Med Biol 2003; 30: 513-9.

[61] Zhang M-R, Maeda J, Ogawa M, *et al*. Development of a new radioligand, N-(5-fluoro-2-phenoxyphenyl)-N-(2-[18F]fluoroethyl-5-methoxybenzyl)acetamide, for pet imaging of peripheral benzodiazepine receptor in primate brain. J Med Chem 2004; 47: 2228-35.

[62] Takano A, Piehl F, Hillert J, *et al. In vivo* TSPO imaging in patients with multiple sclerosis: a brain PET study with [18F]FEDAA1106. EJNMMI Res 2013; 3: 30.

[63] Briard E, Hong J, Musachio JL, Zoghbi SS, Fujita M, Imaizumi M, Cropley V, Innis RB PV. Synthesis and evaluation of two candidate 11C-labeled radioligands for brain peripheral benzodiazepine receptors. J Label Compd Radiopharm 2005; 48: S4.

[64] Briard E, Shah J, Musachio JL, Zoghbi SS, Fujita M, Imaizumi M, Cropley V, Innis RB PV. Synthesis and evaluation of a new 18F-labeled ligand for PET imaging of brain peripheral benzodiazepine receptors. J Label Compd Radiopharm 2005; 48: S4.

[65] Imaizumi M, Briard E, Zoghbi SS, *et al.* Kinetic evaluation in nonhuman primates of two new PET ligands for peripheral benzodiazepine receptors in brain. Synapse 2007; 61: 595-605.

[66] Lartey FM, Ahn G-O, Shen B, *et al.* PET Imaging of Stroke-Induced Neuroinflammation in Mice Using [(18)F]PBR06. Mol Imaging Biol 2013;

[67] Fujimura Y, Zoghbi SS, Simèon FG, *et al.* Quantification of translocator protein (18 kDa) in the human brain with PET and a novel radioligand, (18)F-PBR06. J Nucl Med 2009; 50: 1047-53.

[68] Fujimura Y, Kimura Y, Siméon FG, *et al.* Biodistribution and radiation dosimetry in humans of a new PET ligand, (18)F-PBR06, to image translocator protein (18 kDa). J Nucl Med 2010; 51: 145-9.

[69] Dickstein LP, Zoghbi SS, Fujimura Y, *et al.* Comparison of 18F- and 11C-labeled aryloxyanilide analogs to measure translocator protein in human brain using positron emission tomography. Eur J Nucl Med Mol Imaging 2011; 38: 352-7.

[70] James ML, Fulton RR, Vercoullie J, *et al.* DPA-714, a new translocator protein-specific ligand: synthesis, radiofluorination, and pharmacologic characterization. J Nucl Med 2008; 49: 814-22.

[71] Chauveau F, Van Camp N, Dollé F, *et al*. Comparative evaluation of the translocator protein radioligands 11C-DPA-713, 18F-DPA-714, and 11C-PK11195 in a rat model of acute neuroinflammation. J Nucl Med 2009; 50: 468-76.

[72] Harhausen D, Sudmann V, Khojasteh U, *et al.* Specific imaging of inflammation with the 18 kDa translocator protein ligand DPA-714 in animal models of epilepsy and stroke. PLoS One 2013; 8: e69529.

[73] Arlicot N, Vercouillie J, Ribeiro MJ, *et al.* Initial evaluation in healthy humans of [18F]DPA-714, a potential PET biomarker for neuroinflammation. Nucl Med Biol 2012; 39: 570-8.

[74] Peyronneau M-A, Saba W, Goutal S, *et al.* Metabolism and quantification of [(18)F]DPA-714, a new TSPO positron emission tomography radioligand. Drug Metab Dispos 2013; 41: 122-31.

[75] Corcia P, Tauber C, Vercoullie J, *et al.* Molecular imaging of microglial activation in amyotrophic lateral sclerosis. PLoS One 2012; 7: e52941.

[76] Boutin H, Chauveau F, Thominiaux C, *et al. In vivo* imaging of brain lesions with [(11)C]CLINME, a new PET radioligand of peripheral benzodiazepine receptors. Glia 2007; 55: 1459-68.

[77] Van Camp N, Boisgard R, Kuhnast B, *et al. In vivo* imaging of neuroinflammation: a comparative study between [(18)F]PBR111, [(11)C]CLINME and [(11)C]PK11195 in an acute rodent model. Eur J Nucl Med Mol Imaging 2010; 37: 962-72.

[78] Fookes CJR, Pham TQ, Mattner F, *et al.* Synthesis and biological evaluation of substituted [18F]imidazo[1,2-a]pyridines and [18F]pyrazolo[1,5-a]pyrimidines for the study of the peripheral benzodiazepine receptor using positron emission tomography. J Med Chem 2008; 51: 3700-12.

[79] Dedeurwaerdere S, Callaghan PD, Pham T, *et al.* PET imaging of brain inflammation during early epileptogenesis in a rat model of temporal lobe epilepsy. EJNMMI Res 2012; 2: 60.

[80] Verschuer JD, Towson J, Eberl S, *et al*. Radiation dosimetry of the translocator protein ligands [18F]PBR111 and [18F]PBR102. Nucl Med Biol 2012; 39: 742-53.

[81] Guo Q, Colasanti A, Owen DR, *et al.* Quantification of the Specific Translocator Protein Signal of 18F-PBR111 in Healthy Humans: A Genetic Polymorphism Effect on *In vivo* Binding. J Nucl Med 2013;

[82] Chauveau F, Boutin H, Van Camp N, *et al. In vivo* imaging of neuroinflammation in the rodent brain with [11C]SSR180575, a novel indoleacetamide radioligand of the translocator protein (18 kDa). Eur J Nucl Med Mol Imaging 2011; 38: 509-14.

[83] Vin V, Leducq N, Bono F, Herbert JM. Binding characteristics of SSR180575, a potent and selective peripheral benzodiazepine ligand. Biochem Biophys Res Commun 2003; 310: 785-90.

[84] Wadsworth H, Jones PA, Chau WF, *et al.* [^{18}F]GE-180: a novel fluorine-18 labelled PET tracer for imaging Translocator protein 18 kDa (TSPO). Bioorg Med Chem Lett 2012; 22: 1308-13.

[85] Owen DRJ, Gunn RN, Rabiner EA, *et al.* Mixed-affinity binding in humans with 18-kDa translocator protein ligands. J Nucl Med 2011; 52: 24-32.

[86] Owen DR, Yeo AJ, Gunn RN, *et al.* An 18-kDa translocator protein (TSPO) polymorphism explains differences in binding affinity of the PET radioligand PBR28. J Cereb Blood Flow Metab 2012; 32: 1-5.

[87] Doorduin J, de Vries EFJ, Dierckx RA, Klein HC. PET imaging of the peripheral benzodiazepine receptor: monitoring disease progression and therapy response in neurodegenerative disorders. Curr Pharm Des 2008; 14: 3297-315.

[88] Schweitzer PJ, Fallon BA, Mann JJ, Kumar JSD. PET tracers for the peripheral benzodiazepine receptor and uses thereof. Drug Discov Today 2010; 15: 933-42.

[89] Di Marzo V. The endocannabinoid system: its general strategy of action, tools for its pharmacological manipulation and potential therapeutic exploitation. Pharmacol Res 2009; 60: 77-84.

[90] Lynn AB, Herkenham M. Localization of cannabinoid receptors and nonsaturable high-density cannabinoid binding sites in peripheral tissues of the rat: implications for receptor-mediated immune modulation by cannabinoids. J Pharmacol Exp Ther 1994; 268: 1612-23.

[91] Galiègue S, Mary S, Marchand J, *et al.* Expression of central and peripheral cannabinoid receptors in human immune tissues and leukocyte subpopulations. Eur J Biochem 1995; 232: 54-61.

[92] Benito C, Núñez E, Tolón RM, *et al.* Cannabinoid CB2 receptors and fatty acid amide hydrolase are selectively overexpressed in neuritic plaque-associated glia in Alzheimer's disease brains. J Neurosci 2003; 23: 11136-41.

[93] Fernandez-Ruiz J, Gonzalez S, Romero J, Ramos J. Cannabinoids in neurodegeneration and neuroprotection. 2005.

[94] Klein TW. Cannabinoid-based drugs as anti-inflammatory therapeutics. Nat Rev Immunol 2005; 5: 400-11.

[95] Maresz K, Carrier EJ, Ponomarev ED, Hillard CJ, Dittel BN. Modulation of the cannabinoid CB2 receptor in microglial cells in response to inflammatory stimuli. J Neurochem 2005; 95: 437-45.

[96] Steffens S, Veillard NR, Arnaud C, *et al.* Low dose oral cannabinoid therapy reduces progression of atherosclerosis in mice. Nature 2005; 434: 782-6.

[97] Yiangou Y, Facer P, Durrenberger P, *et al.* COX-2, CB2 and P2X7-immunoreactivities are increased in activated microglial cells/macrophages of multiple sclerosis and amyotrophic lateral sclerosis spinal cord. BMC Neurol 2006; 6: 12.

[98] Iuvone T, De Filippis D, Di Spiezio Sardo A, *et al.* Selective CB2 up-regulation in women affected by endometrial inflammation. J Cell Mol Med 2008; 12: 661-70.

[99] Palazuelos J, Davoust N, Julien B, *et al.* The CB(2) cannabinoid receptor controls myeloid progenitor trafficking: involvement in the pathogenesis of an animal model of multiple sclerosis. J Biol Chem 2008; 283: 13320-9.

[100] Palazuelos J, Aguado T, Pazos MR, *et al.* Microglial CB2 cannabinoid receptors are neuroprotective in Huntington's disease excitotoxicity. Brain 2009; 132: 3152-64.

[101] Sagredo O, González S, Aroyo I, *et al.* Cannabinoid CB2 receptor agonists protect the striatum against malonate toxicity: relevance for Huntington's disease. Glia 2009; 57: 1154-67.

[102] Weis F, Beiras-Fernandez A, Sodian R, *et al.* Substantially altered expression pattern of cannabinoid receptor 2 and activated endocannabinoid system in patients with severe heart failure. J Mol Cell Cardiol 2010; 48: 1187-93.

[103] Martín-Moreno AM, Brera B, Spuch C, *et al.* Prolonged oral cannabinoid administration prevents neuroinflammation, lowers β-amyloid levels and improves cognitive performance in Tg APP 2576 mice. J Neuroinflammation 2012; 9: 8.

[104] Evens N, Bosier B, Lavey BJ, *et al.* Labelling and biological evaluation of [(11)C]methoxy-Sch225336: a radioligand for the cannabinoid-type 2 receptor. Nucl Med Biol 2008; 35: 793-800.

[105] Evens N, Muccioli GG, Houbrechts N, *et al.* Synthesis and biological evaluation of carbon-11- and fluorine-18-labeled 2-oxoquinoline derivatives for type 2 cannabinoid receptor positron emission tomography imaging. Nucl Med Biol 2009; 36: 455-65.

[106] Vandeputte C, Evens N, Toelen J, *et al.* A PET brain reporter gene system based on type 2 cannabinoid receptors. J Nucl Med 2011; 52: 1102-9.

[107] Evens N, Vandeputte C, Coolen C, *et al*. Preclinical evaluation of [11C]NE40, a type 2 cannabinoid receptor PET tracer. Nucl Med Biol 2012; 39: 389-99.

[108] Turkman N, Shavrin A, Ivanov RA, *et al.* Fluorinated cannabinoid CB2 receptor ligands: synthesis and *in vitro* binding characteristics of 2-oxoquinoline derivatives. Bioorg Med Chem 2011; 19: 5698-707.

[109] Turkman N, Shavrin A, Paolillo V, *et al*. Synthesis and preliminary evaluation of [18F]-labeled 2-oxoquinoline derivatives for PET imaging of cannabinoid CB2 receptor. Nucl Med Biol 2012; 39: 593-600.

[110] Horti AG, Gao Y, Ravert HT, *et al*. Synthesis and biodistribution of [11C]A-836339, a new potential radioligand for PET imaging of cannabinoid type 2 receptors (CB2). Bioorg Med Chem 2010; 18: 5202-7.

[111] Evens N, Vandeputte C, Muccioli GG, *et al.* Synthesis, *in vitro* and *in vivo* evaluation of fluorine-18 labelled FE-GW405833 as a PET tracer for type 2 cannabinoid receptor imaging. Bioorg Med Chem 2011; 19: 4499-505.

[112] Fujinaga M, Kumata K, Yanamoto K, *et al.* Radiosynthesis of novel carbon-11-labeled triaryl ligands for cannabinoid-type 2 receptor. Bioorg Med Chem Lett 2010; 20: 1565-8.

[113] Gao M, Wang M, Miller KD, Hutchins GD, Zheng Q-H. Synthesis and *in vitro* biological evaluation of carbon-11-labeled quinoline derivatives as new candidate PET radioligands for cannabinoid CB2 receptor imaging. Bioorg Med Chem 2010; 18: 2099-106.

[114] Rühl T, Deuther-Conrad W, Fischer S, *et al*. Cannabinoid receptor type 2 (CB2)-selective N-aryl-oxadiazolyl-propionamides: synthesis, radiolabelling, molecular modelling and biological evaluation. Org Med Chem Lett 2012; 2: 32.

[115] Teodoro R, Moldovan R-P, Lueg C, *et al.* Radiofluorination and biological evaluation of N-aryl-oxadiazolyl-propionamides as potential radioligands for PET imaging of cannabinoid CB2 receptors. Org Med Chem Lett 2013; 3: 11.

[116] Mu L, Bieri D, Slavik R, *et al.* Radiolabeling and *in vitro* /*in vivo* evaluation of N-(1-adamantyl)-8-methoxy-4-oxo-1-phenyl-1,4-dihydroquinoline-3-carboxamide as a PET probe for imaging cannabinoid type 2 receptor. J Neurochem 2013; 126: 616-24.

[117] Hortala L, Arnaud J, Roux P, *et al.* Synthesis and preliminary evaluation of a new fluorine-18 labelled triazine derivative for PET imaging of cannabinoid CB2 receptor. Bioorg Med Chem Lett 2014; 24: 283-7.

[118] Farooqui AA, Horrocks LA, Farooqui T. Modulation of inflammation in brain: a matter of fat. J Neurochem 2007; 101: 577-99.

[119] McGeer PL, McGeer EG. NSAIDs and Alzheimer disease: epidemiological, animal model and clinical studies. Neurobiol Aging 2007; 28: 639-47.

[120] Vlad SC, Miller DR, Kowall NW, Felson DT. Protective effects of NSAIDs on the development of Alzheimer disease. Neurology 2008; 70: 1672-7.

[121] Breitner JCS, Haneuse SJPA, Walker R, *et al.* Risk of dementia and AD with prior exposure to NSAIDs in an elderly community-based cohort. Neurology 2009; 72: 1899-905.

[122] Hernán MA, Logroscino G, García Rodríguez LA. Nonsteroidal anti-inflammatory drugs and the incidence of Parkinson disease. Neurology 2006; 66: 1097-9.

[123] Wahner AD, Bronstein JM, Bordelon YM, Ritz B. Nonsteroidal anti-inflammatory drugs may protect against Parkinson disease. Neurology 2007; 69: 1836-42.

[124] Esposito E, Di Matteo V, Benigno A, Pierucci M, Crescimanno G, Di Giovanni G. Non-steroidal anti-inflammatory drugs in Parkinson's disease. Exp Neurol 2007; 205: 295-312.

[125] Etminan M, Carleton BC, Samii A. Non-steroidal anti-inflammatory drug use and the risk of Parkinson disease: a retrospective cohort study. J Clin Neurosci 2008; 15: 576-7.

[126] Bosetti F, Langenbach R, Weerasinghe GR. Prostaglandin E2 and microsomal prostaglandin E synthase-2 expression are decreased in the cyclooxygenase-2-deficient mouse brain despite compensatory induction of cyclooxygenase-1 and Ca2+-dependent phospholipase A2. J Neurochem 2004; 91: 1389-97.

[127] Murakami M, Kudo I. Recent advances in molecular biology and physiology of the prostaglandin E2-biosynthetic pathway. Prog Lipid Res 2004; 43: 3-35.

[128] Choi S-H, Langenbach R, Bosetti F. Cyclooxygenase-1 and -2 enzymes differentially regulate the brain upstream NF-kappa B pathway and downstream enzymes involved in prostaglandin biosynthesis. J Neurochem 2006; 98: 801-11.

[129] Chandrasekharan N V, Dai H, Roos KLT, *et al.* COX-3, a cyclooxygenase-1 variant inhibited by acetaminophen and other analgesic/antipyretic drugs: cloning, structure, and expression. Proc Natl Acad Sci U S A 2002; 99: 13926-31.

[130] Phillis JW, Horrocks LA, Farooqui AA. Cyclooxygenases, lipoxygenases, and epoxygenases in CNS: their role and involvement in neurological disorders. Brain Res Rev 2006; 52: 201-43.

[131] Tzeng S-F, Hsiao H-Y, Mak O-T. Prostaglandins and cyclooxygenases in glial cells during brain inflammation. Curr Drug Targets Inflamm Allergy 2005; 4: 335-40.

[132] Greenhough A, Smartt HJM, Moore AE, *et al.* The COX-2/PGE2 pathway: key roles in the hallmarks of cancer and adaptation to the tumour microenvironment. Carcinogenesis 2009; 30: 377-86.

[133] Wang D, Dubois RN. Eicosanoids and cancer. Nat Rev Cancer 2010; 10: 181-93.

[134] Rizzo MT. Cyclooxygenase-2 in oncogenesis. Clin Chim Acta 2011; 412: 671-87.

[135] Kniess T, Laube M, Bergmann R, *et al.* Radiosynthesis of a ^{18}F-labeled 2,3-diarylsubstituted indole via McMurry coupling for functional characterization of cyclooxygenase-2 (COX-2) *in vitro* and *in vivo*. Bioorg Med Chem 2012; 20: 3410-21.

[136] Niwa K, Araki E, Morham SG, Ross ME, Iadecola C. Cyclooxygenase-2 contributes to functional hyperemia in whisker-barrel cortex. J Neurosci 2000; 20: 763-70.

[137] Yang H, Chen C. Cyclooxygenase-2 in synaptic signaling. Curr Pharm Des 2008; 14: 1443-51.

[138] Schwab JM, Beschorner R, Meyermann R, Gözalan F, Schluesener HJ. Persistent accumulation of cyclooxygenase-1-expressing microglial cells and macrophages and transient upregulation by endothelium in human brain injury. J Neurosurg 2002; 96: 892-9.

[139] Pepicelli O, Fedele E, Berardi M, *et al.* Cyclo-oxygenase-1 and -2 differently contribute to prostaglandin E2 synthesis and lipid peroxidation after *in vivo* activation of N-methyl-D-aspartate receptors in rat hippocampus. J Neurochem 2005; 93: 1561-7.

[140] Candelario-Jalil E, de Oliveira ACP, Gräf S, *et al.* Resveratrol potently reduces prostaglandin E2 production and free radical formation in lipopolysaccharide-activated primary rat microglia. J Neuroinflammation 2007; 4: 25.

[141] Choi S-H, Langenbach R, Bosetti F. Genetic deletion or pharmacological inhibition of cyclooxygenase-1 attenuate lipopolysaccharide-induced inflammatory response and brain injury. FASEB J 2008; 22: 1491-501.

[142] Shukuri M, Takashima-Hirano M, Tokuda K, *et al. In vivo* expression of cyclooxygenase-1 in activated microglia and macrophages during neuroinflammation visualized by PET with 11C-ketoprofen methyl ester. J Nucl Med 2011; 52: 1094-101.

[143] Schwab JM, Nguyen TD, Postler E, Meyermann R, Schluesener HJ. Selective accumulation of cyclooxygenase-1-expressing microglial cells/macrophages in lesions of human focal cerebral ischemia. Acta Neuropathol 2000; 99: 609-14.

[144] Minghetti L. Role of COX-2 in inflammatory and degenerative brain diseases. Subcell Biochem 2007; 42: 127-41.

[145] Hoozemans JJM, Rozemuller JM, van Haastert ES, Veerhuis R, Eikelenboom P. Cyclooxygenase-1 and -2 in the different stages of Alzheimer's disease pathology. Curr Pharm Des 2008; 14: 1419-27.

[146] Choi S-H, Aid S, Bosetti F. The distinct roles of cyclooxygenase-1 and -2 in neuroinflammation: implications for translational research. Trends Pharmacol Sci 2009; 30: 174-81.

[147] Channing M, Simpson N. Radiosynthesis of 1-[C11] polyhomoallylic fatty-acids. J Label Compd Rad 1993; 33: 541-6.

[148] Rapoport SI. *In vivo* approaches to quantifying and imaging brain arachidonic and docosahexaenoic acid metabolism. J Pediatr 2003; 143: S26-34.

[149] De Vries EFJ. Imaging of cyclooxygenase-2 (COX-2) expression: potential use in diagnosis and drug evaluation. Curr Pharm Des 2006; 12: 3847-56.

[150] McCarthy TJ, Sheriff AU, Graneto MJ, Talley JJ, Welch MJ. Radiosynthesis, *in vitro* validation, and *in vivo* evaluation of 18F-labeled COX-1 and COX-2 inhibitors. J Nucl Med 2002; 43: 117-24.

[151] De Vries EFJ, van Waarde A, Buursma AR, Vaalburg W. Synthesis and *in vivo* evaluation of 18F-desbromo-DuP-697 as a PET tracer for cyclooxygenase-2 expression. J Nucl Med 2003; 44: 1700-6.

[152] Toyokuni T, Kumar JSD, Walsh JC, *et al.* Synthesis of 4-(5-[18F]fluoromethyl-3-phenylisoxazol-4-yl)benzenesulfonamide, a new [18F]fluorinated analogue of valdecoxib, as a potential radiotracer for imaging cyclooxygenase-2 with positron emission tomography. Bioorg Med Chem Lett 2005; 15: 4699-702.

[153] Prabhakaran J, Underwood MD, Parsey R V, *et al.* Synthesis and *in vivo* evaluation of [18F]-4-[5-(4-methylphenyl)-3-(trifluoromethyl)-1H-pyrazol-1-yl]benzenesulfonamide as a PET imaging probe for COX-2 expression. Bioorg Med Chem 2007; 15: 1802-7.

[154] De Vries EFJ, Doorduin J, Dierckx RA, van Waarde A. Evaluation of [(11)C]rofecoxib as PET tracer for cyclooxygenase 2 overexpression in rat models of inflammation. Nucl Med Biol 2008; 35: 35-42.

[155] Comley R, Passchier J, Willemsen A, *et al.* Uptake and regional distribution of [11C]rofecoxib in the human brain. 2010.

[156] Uddin MJ, Crews BC, Ghebreselasie K, *et al.* Fluorinated COX-2 inhibitors as agents in PET imaging of inflammation and cancer. Cancer Prev Res (Phila) 2011; 4: 1536-45.

[157] Takashima-Hirano M, Shukuri M, Takashima T, *et al.* General method for the (11)C-labeling of 2-arylpropionic acids and their esters: construction of a PET tracer library for a study of biological events involved in COXs expression. Chemistry 2010; 16: 4250-8.

[158] Parks WC, Wilson CL, López-Boado YS. Matrix metalloproteinases as modulators of inflammation and innate immunity. Nat Rev Immunol 2004; 4: 617-29.

[159] Wagner S, Breyholz H-J, Faust A, *et al.* Molecular imaging of matrix metalloproteinases *in vivo* using small molecule inhibitors for SPECT and PET. Curr Med Chem 2006; 13: 2819-38.

[160] Galis ZS, Khatri JJ. Matrix metalloproteinases in vascular remodeling and atherogenesis: the good, the bad, and the ugly. Circ Res 2002; 90: 251-62.

[161] Iwama S, Sugimura Y, Suzuki H, *et al.* Time-dependent changes in proinflammatory and neurotrophic responses of microglia and astrocytes in a rat model of osmotic demyelination syndrome. Glia 2011; 59: 452-62.

[162] Siasos G, Tousoulis D, Kioufis S, *et al.* Inflammatory mechanisms in atherosclerosis: the impact of matrix metalloproteinases. Curr Top Med Chem 2012; 12: 1132-48.

[163] Wagner S, Breyholz H-J, Law MP, *et al.* Novel fluorinated derivatives of the broad-spectrum MMP inhibitors N-hydroxy-2(R)-[[(4-methoxyphenyl)sulfonyl](benzyl)- and (3-picolyl)-amino]-3-methyl-butanamide as potential tools for the molecular imaging of activated MMPs with PET. J Med Chem 2007; 50: 5752-64.

[164] Vos CMP, van Haastert ES, de Groot CJA, van der Valk P, de Vries HE. Matrix metalloproteinase-12 is expressed in phagocytotic macrophages in active multiple sclerosis lesions. J Neuroimmunol 2003; 138: 106-14.

[165] Nuttall RK, Silva C, Hader W, *et al.* Metalloproteinases are enriched in microglia compared with leukocytes and they regulate cytokine levels in activated microglia. Glia 2007; 55: 516-26.

[166] Dasilva AG, Yong VW. Expression and regulation of matrix metalloproteinase-12 in experimental autoimmune encephalomyelitis and by bone marrow derived macrophages *in vitro*. J Neuroimmunol 2008; 199: 24-34.

[167] Crocker SJ, Frausto RF, Whitton JL, Milner R. A novel method to establish microglia-free astrocyte cultures: comparison of matrix metalloproteinase expression profiles in pure cultures of astrocytes and microglia. Glia 2008; 56: 1187-98.

[168] Liu Y, Zhang M, Hao W, *et al.* Matrix metalloproteinase-12 contributes to neuroinflammation in the aged brain. Neurobiol Aging 2013; 34: 1231-9.

[169] Yong VW. Metalloproteinases: mediators of pathology and regeneration in the CNS. Nat Rev Neurosci 2005; 6: 931-44.

[170] Breyholz HJ, Wagner S, Levkau B, Schober O, Schäfers M, Kopka K. A 18F-radiolabeled analogue of CGS 27023A as a potential agent for assessment of matrix-metalloproteinase activity *in vivo*. Q J Nucl Med Mol imaging Off Publ Ital Assoc Nucl Med [and] Int Assoc Radiopharmacol (IAR), [and] Sect Soc Radiopharm 2007; 51: 24-32.

[171] Breyholz H-J, Wagner S, Faust A, *et al.* Radiofluorinated pyrimidine-2,4,6-triones as molecular probes for noninvasive MMP-targeted imaging. ChemMedChem 2010; 5: 777-89.

[172] Schrigten D, Breyholz H-J, Wagner S, *et al.* A new generation of radiofluorinated pyrimidine-2,4,6-triones as MMP-targeted radiotracers for positron emission tomography. J Med Chem 2012; 55: 223-32.

[173] Hugenberg V, Breyholz H-J, Riemann B, *et al.* A new class of highly potent matrix metalloproteinase inhibitors based on triazole-substituted hydroxamates: (radio)synthesis and *in vitro* and first *in vivo* evaluation. J Med Chem 2012; 55: 4714-27.

[174] Bergström M, Muhr C, Jossan S, Lilja A, Nyberg G, Långström B. Differentiation of pituitary adenoma and meningioma: visualization with positron emission tomography and [11C]-L-deprenyl. Neurosurgery 1992; 30: 855-61.

[175] Fowler JS, Volkow ND, Logan J, *et al.* Monoamine oxidase B (MAO B) inhibitor therapy in Parkinson's disease: the degree and reversibility of human brain MAO B inhibition by Ro 19 6327. Neurology 1993; 43: 1984-92.

[176] Kumlien E, Bergström M, Lilja A, *et al.* Positron emission tomography with [11C]deuterium-deprenyl in temporal lobe epilepsy. Epilepsia 1995; 36: 712-21.

[177] Kumlien E, Nilsson A, Hagberg G, Långström B, Bergström M. PET with 11C-deuterium-deprenyl and 18F-FDG in focal epilepsy. Acta Neurol Scand 2001; 103: 360-6.

[178] Fowler JS, Volkow ND, Cilento R, Wang GJ, Felder C, Logan J. Comparison of Brain Glucose Metabolism and Monoamine Oxidase B (MAO B) in Traumatic Brain Injury. Clin Positron Imaging 1999; 2: 71-9.

[179] Johansson A, Engler H, Blomquist G, *et al.* Evidence for astrocytosis in ALS demonstrated by [11C](L)-deprenyl-D2 PET. J Neurol Sci 2007; 255: 17-22.

[180] Razifar P, Axelsson J, Schneider H, Långström B, Bengtsson E, Bergström M. A new application of pre-normalized principal component analysis for improvement of image quality and clinical diagnosis in human brain PET studies--clinical brain studies using [11C]-GR205171, [11C]-L-deuterium-deprenyl, [11C]-5-Hydroxy-L-Tryptophan, [11. Neuroimage 2006; 33: 588-98.

[181] Saba W, Valette H, Peyronneau M-A, *et al.* [(11)C]SL25.1188, a new reversible radioligand to study the monoamine oxidase type B with PET: preclinical characterisation in nonhuman primate. Synapse 2010; 64: 61-9.

[182] Vasdev N, Sadovski O, Moran MD, *et al.* Development of new radiopharmaceuticals for imaging monoamine oxidase B. Nucl Med Biol 2011; 38: 933-43.

[183] Nag S, Lehmann L, Heinrich T, *et al.* Synthesis of three novel fluorine-18 labeled analogues of L-deprenyl for positron emission tomography (PET) studies of monoamine oxidase B (MAO-B). J Med Chem 2011; 54: 7023-9.

[184] Nag S, Varrone A, Tóth M, *et al. In vivo* evaluation in cynomolgus monkey brain and metabolism of [^{18}F]fluorodeprenyl: a new MAO-B pet radioligand. Synapse 2012; 66: 323-30.

[185] Nag S, Lehmann L, Kettschau G, *et al.* Synthesis and evaluation of [^{18}F]fluororasagiline, a novel positron emission tomography (PET) radioligand for monoamine oxidase B (MAO-B). Bioorg Med Chem 2012; 20: 3065-71.

[186] Nag S, Kettschau G, Heinrich T, *et al.* Synthesis and biological evaluation of novel propargyl amines as potential fluorine-18 labeled radioligands for detection of MAO-B activity. Bioorg Med Chem 2013; 21: 186-95.

[187] Monif M, Burnstock G, Williams DA. Microglia: proliferation and activation driven by the P2X7 receptor. Int J Biochem Cell Biol 2010; 42: 1753-6.

[188] Skaper SD, Debetto P, Giusti P. The P2X7 purinergic receptor: from physiology to neurological disorders. FASEB J 2010; 24: 337-45.

[189] Parvathenani LK, Tertyshnikova S, Greco CR, Roberts SB, Robertson B, Posmantur R. P2X7 mediates superoxide production

in primary microglia and is up-regulated in a transgenic mouse model of Alzheimer's disease. J Biol Chem 2003; 278: 13309-17.

[190] Romagnoli R, Baraldi PG, Cruz-Lopez O, *et al*. The P2X7 receptor as a therapeutic target. Expert Opin Ther Targets 2008; 12: 647-61.

[191] Sanz JM, Chiozzi P, Ferrari D, *et al*. Activation of microglia by amyloid {beta} requires P2X7 receptor expression. J Immunol 2009; 182: 4378-85.

[192] Takenouchi T, Sekiyama K, Sekigawa A, *et al*. P2X7 receptor signaling pathway as a therapeutic target for neurodegenerative diseases. Arch Immunol Ther Exp (Warsz) 2010; 58: 91-6.

[193] Diaz-Hernandez JI, Gomez-Villafuertes R, León-Otegui M, *et al*. *In vivo* P2X7 inhibition reduces amyloid plaques in Alzheimer's disease through GSK3β and secretases. Neurobiol Aging 2012; 33: 1816-28.

[194] Honore P, Donnelly-Roberts D, Namovic MT, *et al*. A-740003 [N-(1-{[(cyanoimino)(5-quinolinylamino) methyl]amino}-2,2-dimethylpropyl)-2-(3,4-dimethoxyphenyl)acetamide], a novel and selective P2X7 receptor antagonist, dose-dependently reduces neuropathic pain in the rat. J Pharmacol Exp Ther 2006; 319: 1376-85.

[195] Donnelly-Roberts DL, Jarvis MF. Discovery of P2X7 receptor-selective antagonists offers new insights into P2X7 receptor function and indicates a role in chronic pain states. Br J Pharmacol 2007; 151: 571-9.

[196] Nelson DW, Gregg RJ, Kort ME, *et al*. Structure-activity relationship studies on a series of novel, substituted 1-benzyl-5-phenyltetrazole P2X7 antagonists. J Med Chem 2006; 49: 3659-66.

[197] Carroll WA, Kalvin DM, Perez Medrano A, *et al*. Novel and potent 3-(2,3-dichlorophenyl)-4-(benzyl)-4H-1,2,4-triazole P2X7 antagonists. Bioorg Med Chem Lett 2007; 17: 4044-8.

[198] McGaraughty S, Chu KL, Namovic MT, *et al*. P2X7-related modulation of pathological nociception in rats. Neuroscience 2007; 146: 1817-28.

[199] Florjancic AS, Peddi S, Perez-Medrano A, *et al*. Synthesis and *in vitro* activity of 1-(2,3-dichlorophenyl)-N-(pyridin-3-ylmethyl)-1H-1,2,4-triazol-5-amine and 4-(2,3-dichlorophenyl)-N-(pyridin-3-ylmethyl)-4H-1,2,4-triazol-3-amine P2X7 antagonists. Bioorg Med Chem Lett 2008; 18: 2089-92.

[200] Gunosewoyo H, Guo JL, Bennett MR, Coster MJ, Kassiou M. Cubyl amides: novel P2X7 receptor antagonists. Bioorg Med Chem Lett 2008; 18: 3720-3.

[201] Carroll WA, Donnelly-Roberts D, Jarvis MF. Selective P2X(7) receptor antagonists for chronic inflammation and pain. Purinergic Signal 2009; 5: 63-73.

[202] Perez-Medrano A, Donnelly-Roberts DL, Honore P, *et al*. Discovery and biological evaluation of novel cyanoguanidine P2X(7) antagonists with analgesic activity in a rat model of neuropathic pain. J Med Chem 2009; 52: 3366-76.

[203] Able SL, Fish RL, Bye H, *et al*. Receptor localization, native tissue binding and ex vivo occupancy for centrally penetrant P2X7 antagonists in the rat. Br J Pharmacol 2011; 162: 405-14.

[204] Gunosewoyo H, Coster MJ, Kassiou M. Molecular probes for P2X7 receptor studies. Curr Med Chem 2007; 14: 1505-23.

[205] Donnelly-Roberts DL, Namovic MT, Surber B, *et al*. [3H]A-804598 ([3H]2-cyano-1-[(1S)-1-phenylethyl]-3-quinolin-5-ylguanidine) is a novel, potent, and selective antagonist radioligand for P2X7 receptors. Neuropharmacology 2009; 56: 223-9.

[206] Beswick PJ, Billinton A, Chambers LJ, *et al*. Structure-activity relationships and *in vivo* activity of (1H-pyrazol-4-yl)acetamide antagonists of the P2X(7) receptor. Bioorg Med Chem Lett 2010; 20: 4653-6.

[207] Abberley L, Bebius A, Beswick PJ, *et al*. Identification of 2-oxo-N-(phenylmethyl)-4-imidazolidinecarboxamide antagonists of the P2X(7) receptor. Bioorg Med Chem Lett 2010; 20: 6370-4.

[208] Abdi MH, Beswick PJ, Billinton A, *et al*. Discovery and structure-activity relationships of a series of pyroglutamic acid amide antagonists of the P2X7 receptor. Bioorg Med Chem Lett 2010; 20: 5080-4.

[209] Gleave RJ, Walter DS, Beswick PJ, *et al*. Synthesis and biological activity of a series of tetrasubstituted-imidazoles as P2X(7) antagonists. Bioorg Med Chem Lett 2010; 20: 4951-4.

[210] Matasi JJ, Brumfield S, Tulshian D, *et al*. Synthesis and SAR development of novel P2X7 receptor antagonists for the treatment of pain: part 1. Bioorg Med Chem Lett 2011; 21: 3805-8.

[211] Duplantier AJ, Dombroski MA, Subramanyam C, *et al*. Optimization of the physicochemical and pharmacokinetic attributes in a 6-azauracil series of P2X7 receptor antagonists leading to the discovery of the clinical candidate CE-224,535. Bioorg Med Chem Lett 2011; 21: 3708-11.

[212] Subramanyam C, Duplantier AJ, Dombroski MA, *et al*. Discovery, synthesis and SAR of azinyl- and azolylbenzamides antagonists of the $P2X_7$ receptor. Bioorg Med Chem Lett 2011; 21: 5475-9.

[213] Brumfield S, Matasi JJ, Tulshian D, *et al*. Synthesis and SAR development of novel P2X7 receptor antagonists for the treatment of pain: part 2. Bioorg Med Chem Lett 2011; 21: 7287-90.

[214] Lee GE, Lee W-G, Lee S-Y, *et al*. Characterization of protoberberine analogs employed as novel human P2X7 receptor antagonists. Toxicol Appl Pharmacol 2011; 252: 192-200.

[215] Lee W-G, Lee S-D, Cho J-H, *et al*. Structure-activity relationships and optimization of 3,5-dichloropyridine derivatives as novel P2X(7) receptor antagonists. J Med Chem 2012; 55: 3687-98.

[216] Letavic MA, Lord B, Bischoff F, *et al*. Synthesis and Pharmacological Characterization of Two Novel, Brain Penetrating P2X 7 Antagonists. ACS Med Chem Lett 2013; 4: 419-22.

[217] Bhattacharya A, Wang Q, Ao H, *et al*. Pharmacological characterization of a novel centrally permeable P2X7 receptor antagonist: JNJ-47965567. Br J Pharmacol 2013; 170: 624-40.

[218] Guile SD, Alcaraz L, Birkinshaw TN, *et al*. Antagonists of the P2X(7) receptor. From lead identification to drug development. J Med Chem 2009; 52: 3123-41.

[219] Gunosewoyo H, Kassiou M. P2X purinergic receptor ligands: recently patented compounds. Expert Opin Ther Pat 2010; 20: 625-46.

[220] Akdis CA, Simons FER. Histamine receptors are hot in immunopharmacology. Eur J Pharmacol 2006; 533: 69-76.

[221] Parsons ME, Ganellin CR. Histamine and its receptors. Br J Pharmacol 2006; 147 Suppl S127-35.

[222] Celanire S, Wijtmans M, Talaga P, Leurs R, de Esch IJP. Keynote review: histamine H3 receptor antagonists reach out for the clinic. Drug Discov Today 2005; 10: 1613-27.

[223] Esbenshade TA, Browman KE, Bitner RS, Strakhova M, Cowart MD, Brioni JD. The histamine H3 receptor: an attractive target for the treatment of cognitive disorders. Br J Pharmacol 2008; 154: 1166-81.

[224] Leurs R, Chazot PL, Shenton FC, Lim HD, de Esch IJP. Molecular and biochemical pharmacology of the histamine H4 receptor. Br J Pharmacol 2009; 157: 14-23.

[225] Zampeli E, Tiligada E. The role of histamine H4 receptor in immune and inflammatory disorders. Br J Pharmacol 2009; 157: 24-33.

[226] Strakhova MI, Cuff CA, Manelli AM, *et al*. *In vitro* and *in vivo* characterization of A-940894: a potent histamine H4 receptor antagonist with anti-inflammatory properties. Br J Pharmacol 2009; 157: 44-54.

[227] Sander K, Kottke T, Proschak E, *et al*. Lead identification and optimization of diaminopyrimidines as histamine H4 receptor ligands. Inflamm Res 2010; 59 Suppl 2: S249-51.

[228] Savall BM, Gomez L, Chavez F, *et al*. Tricyclic aminopyrimidine histamine H4 receptor antagonists. Bioorg Med Chem Lett 2011; 21: 6577-81.

[229] Mowbray CE, Bell AS, Clarke NP, *et al*. Challenges of drug discovery in novel target space. The discovery and evaluation of PF-3893787: a novel histamine H4 receptor antagonist. Bioorg Med Chem Lett 2011; 21: 6596-602.

[230] Lane CAL, Hay D, Mowbray CE, *et al*. Synthesis of novel histamine H4 receptor antagonists. Bioorg Med Chem Lett 2012; 22: 1156-9.

[231] Funke U, Vugts DJ, Janssen B, *et al*. (11) C-labeled and (18) F-labeled PET ligands for subtype-specific imaging of histamine receptors in the brain. J Labelled Comp Radiopharm 2013; 56: 120-9.

Received: May 9, 2014 **Accepted: June 12, 2014**